2019 Outfall Benthic Monitoring Results

Massachusetts Water Resources Authority
Environmental Quality Department
Report 2020-10

Citation:

Nestler EC, Diaz RJ, Madray ME. 2020. **2019 Outfall Benthic Monitoring Results**. Boston: Massachusetts Water Resources Authority. Report 2020-10. 65 p.

Environmental Quality Department reports can be downloaded from
http://www.mwra.com/harbor/enquad/trlist.html

2019 Outfall Benthic Monitoring Results

Submitted to

Massachusetts Water Resources Authority
Environmental Quality Department
100 First Avenue
Charlestown Navy Yard
Boston, MA 02129
(617) 242-6000

Prepared by

Eric C.Nestler[1]
Robert J. Diaz[2]
Maureen E. Madray[1]

[1]Normandeau Associates, Inc.
25 Nashua Road
Bedford, NH 30110

[2]Diaz and Daughters
6198 Driftwood Lane
Ware Neck, VA 23178

November 2020

Environmental Quality Report No. 2020-10

TABLE OF CONTENTS

PAGE

EXECUTIVE SUMMARY 6
1 INTRODUCTION 8
2 METHODS 9
2.1 FIELD METHODS 9
2.2 LABORATORY METHODS 12
2.3 DATA HANDLING, REDUCTION, AND ANALYSIS 12
2.3.1 Data Reduction and Statistics for SPI Images 13
3 RESULTS AND DISCUSSION 14
3.1 SEDIMENT CONDITIONS 14
3.1.1 *Clostridium perfringens*, Grain Size, and Total Organic Carbon 14
3.2 BENTHIC INFAUNA 20
3.2.1 Community Parameters 20
3.2.2 Infaunal Assemblages 24
3.3 SEDIMENT PROFILE IMAGING 28
4 SUMMARY OF RELEVANCE TO MONITORING OBJECTIVES 60
5 REFERENCES 62

FIGURES

PAGE

Figure 2-1. Locations of soft-bottom sampling stations for 2019. 10
Figure 2-2. Locations of sediment profile imaging stations for 2019. 11
Figure 3-1. Mean concentrations of *Clostridium perfringens* in four areas of Massachusetts Bay, 1992 to 2019. 16
Figure 3-2. Monitoring results for *Clostridium perfringens* in 2019. 16
Figure 3-3. Monitoring results for sediment grain size in 2019. 17
Figure 3-4. Mean percent fine sediments at FF01A, FF04, NF12 and NF17; 1992 to 2019. 17
Figure 3-5. Mean concentrations of TOC at four stations in Massachusetts Bay, 1992 to 2019. 18
Figure 3-8. Mean (with 95% confidence intervals) concentrations of TOC at four areas in Massachusetts Bay during the baseline (1992-2000) and post-diversion (2001 to 2018) compared to 2019. 19
Figure 3-9. Mean infaunal abundance per sample at four areas of Massachusetts Bay, 1992 to 2019. 22
Figure 3-10. Mean number of species per sample at four areas of Massachusetts Bay, 1992 to 2019. 22
Figure 3-11. Mean (and 95% confidence intervals) Shannon-Wiener Diversity (H′) at nearfield stations in comparison to threshold limit, 1992 to 2019. 23
Figure 3-12. Mean (and 95% confidence intervals) Pielou's Evenness (J′) at nearfield stations in comparison to threshold limit, 1992 to 2019. 23
Figure 3-13. Results of cluster analysis of the 2019 infauna samples. 25
Figure 3-14. Results of a MDS ordination of the 2019 infauna samples from Massachusetts Bay showing distance from the outfall. 25
Figure 3-15. Percent fine sediments superimposed on the MDS ordination plot of the 2019 infauna samples. 26
Figure 3-16. Trends in apparent color redox-potential discontinuity (aRPD) layer depth and organism sediment index (OSI) through time. 34
Figure 3-17. Trends in SPI parameters and grain-size through time. 35
Figure 3-18. Conceptual model of major driving factors effecting benthic and pelagic ecosystems in the nearfield monitoring area. 36
Figure 3-19. Long-term climate driven changes in winter-period (October to May) storm intensity and number from 1990 to 2018 (Codiga et al. 2019). 37
Figure 3-20. Long-term climate driven changes in temperature and salinity (MWRA monitoring database). 38
Figure 3-21. Matrix of estimated successional stage through time. Stations are arranged from coarsest to finest sediments. 39
Figure 3-22. Relationships between winter-period storms, and SPI and sediment parameters. 40

Figure 3-23. Shift in dominance of processes structuring surface sediments at station FF13 through time. 41
Figure 3-24. Mosaic of SPI images for Station NF17 where sediments coarsened thought time. 42
Figure 3-25. Coarsening of modal from SPI images and median sediment grain-size from grab samples at Station NF17. 43
Figure 3-26. Mosaic of SPI images for Station NF12 with mixed fine-sand-silt-clay sediments. 44
Figure 3-27 Total infaunal abundance at Station NF17 and relationships with storm intensity. Green line is two-year moving average. 45
Figure 3-28 Abundance patterns for top six species at sandy Station NF17. 46
Figure 3-29 Relationships between abundance and winter-period storm intensity for top six species at sandy Station NF17. 47
Figure 3-30 Tubes of the amphipod Crassicorophium crassicorne at sandy Station NF17. 48
Figure 3-31 Total infaunal abundance at Station NF12 and relationships with storm intensity. Green line is two-year moving average. 49
Figure 3-32 Abundance patterns for top six species at mixed sediment Station NF12. 50
Figure 3-33 Relationships between abundance and winter-period storm intensity for top six species at mixed sediment Station NF12. 51
Figure 3-34 Abundance of Prionospio steenstrupi at mixed sediment Station NF12. 52
Figure 3-35 Percent fines at nearfield stations for all years (1991 to 2019) arranged from highest to lowest. 55
Figure 3-36 Relationship between percent fines, median Phi, and total organic carbon (TOC) for all nearfield station-year combinations. 56
Figure 3-37 Abundance of six top dominants at muddy stations. 57
Figure 3-38 Abundance of six top dominants at sand (medium-to coarse-sand) stations. 58

TABLES

PAGE

Table 3-1. Monitoring results for sediment condition parameters in 2019. 15
Table 3-2. Monitoring results for infaunal community parameters in 2019. 21
Table 3-3. Infaunal monitoring threshold results, August 2019 samples. 21
Table 3-4. Abundance (mean # per grab) of numerically dominant taxa (10 most abundant per group) composing infaunal assemblages identified by cluster analysis of the 2019 samples. 27
Table 3-5. Summary of SPI parameters pre- and post-baseline years for all nearfield stations. 33
Table 3-6. Correlation (r) of sediment parameters for all 23 stations over the 28 years of monitoring. 53
Table 3-7. Correlation (r) of the six top dominant species at muddy Station NF12 and six at sandy Station NF17 with sediment parameters from all 23 stations over the 28 years of monitoring. 54

EXECUTIVE SUMMARY

The Massachusetts Water Resources Authority (MWRA) has conducted long-term monitoring since 1992 in Massachusetts Bay and Cape Cod Bay to evaluate the potential effects of discharging secondary treated effluent 15 kilometers (km) offshore in Massachusetts Bay. Relocation of the outfall from Boston Harbor to Massachusetts Bay in September 2000 raised concerns about potential effects of the discharge on the offshore benthic (bottom) environment, which are addressed by the results reported here.

Benthic monitoring during 2019 included soft-bottom sampling for sediments and infauna at 14 nearfield and farfield stations, and sediment profile imaging (SPI) at 23 nearfield stations.

Sediment conditions were characterized based on spore counts of the anaerobic bacterium, *Clostridium perfringens*, analyses of sediment grain size composition and total organic carbon (TOC). *C. perfringens* concentrations during 2019 were highest at sites closest to the discharge. These findings are consistent with those obtained since outfall relocation (e.g. Rutecki et al. 2019, Maciolek et al. 2007, 2008). The results for *C. perfringens*, therefore, provide evidence of settlement of solids from the effluent at sites in close proximity (within 2 km) to the outfall. Neither sediment grain size nor TOC have exhibited appreciable changes from the baseline period and this pattern continued in 2019. These results indicate the absence of influence of the wastewater discharge on sediment conditions beyond *Clostridium* spores, consistent with prior monitoring results (Rutecki et al. 2019, Nestler et al. 2018, Maciolek et al. 2008).

As seen in previous years, there was no evidence of impacts to the infaunal communities in Massachusetts Bay from the offshore outfall in 2019. Monitoring results have consistently suggested that deposition of particulate organic matter from the wastewater discharge is not occurring at levels that disturb or smother animals near the outfall. There were no Contingency Plan threshold exceedances for any infaunal diversity measures in 2019. Multivariate analyses indicated that patterns in the distribution of faunal assemblages reflect habitat types at the sampling stations. Infaunal data in 2019 continue to suggest that the macrobenthic communities at sampling stations near the outfall have not been adversely impacted by the wastewater discharge.

The 2019 SPI survey found no indication that the wastewater discharge has resulted in low levels of dissolved oxygen in nearfield sediments. The average thickness of the sediment oxic layer in 2019 was greater than during the baseline period and among the highest reported during post-discharge years. These results support previous findings that organic loading and an associated decrease in oxygen levels have not been a problem at the nearfield benthic monitoring stations (Rutecki et al. 2019, Maciolek et al. 2008). The findings also support MWRA's recommendation to regulatory agencies and their Outfall Monitoring Science Advisory Panel (OMSAP) that the SPI study in Massachusetts Bay had answered its monitoring questions fully and could be ended. OMSAP endorsed this recommendation at their October 3, 2019 meeting.

Rutecki et al. (2019) included an assessment of regional storminess during sediment monitoring that began in 1992, and tested whether there is evidence that storms are impacting the benthos. That assessment strongly supported that the trend seen in the SPI results likely resulted from the coarsening of sediment grain-size caused by sediment mixing and transport associated with storms that produced a

decline in visible biogenic structures in the images. Further analyses with 2019 data also support that conclusion.

The outfall is located in an area dominated by hydrodynamic and physical factors, including tidal and storm currents, turbulence, and sediment transport (Butman et al. 2008). These physical factors, combined with the high quality of the effluent discharged into the Bay (Taylor 2010, Werme et al. 2019), are the principal reasons that benthic habitat quality has remained high in the nearfield area.

1 INTRODUCTION

The Massachusetts Water Resources Authority (MWRA) has conducted long-term monitoring since 1992 in Massachusetts Bay and Cape Cod Bay to evaluate the potential effects of discharging secondary treated effluent 15 kilometers (km) offshore in Massachusetts Bay. Relocation of the outfall from Boston Harbor to Massachusetts Bay in September 2000 raised concerns about potential effects of the discharge on the offshore benthic (bottom) environment. These concerns focused on three issues: (1) eutrophication and related low levels of dissolved oxygen; (2) accumulation of toxic contaminants in depositional areas; and (3) smothering of animals by particulate matter.

Under its Ambient Monitoring Plan (MWRA 1991, 1997, 2001, 2004, 2010) the MWRA has collected extensive information over a nine-year baseline period (1992–2000) and a nineteen-year post-diversion period (2001–2019). These studies include surveys of sediments and soft-bottom communities using traditional grab sampling and sediment profile imaging (SPI) as well as surveys of hard-bottom communities using a remotely operated vehicle (ROV). Data collected by this program allow for a more complete understanding of the bay system and provide a basis to explain any changes in benthic conditions and to address the question of whether MWRA's discharge has contributed to any such changes.

Benthic monitoring during 2019 was conducted following the current Ambient Monitoring Plan (MWRA 2010) which is required under MWRA's effluent discharge permit for the Deer Island Treatment Plant. Under this plan, annual monitoring includes soft-bottom sampling for sediment conditions and infauna at 14 nearfield and farfield stations, and Sediment Profile Imaging (SPI) at 23 nearfield stations. Every third year, sediment contaminants are evaluated (at the same 14 stations where infauna and sediment condition samples are collected) and hard-bottom surveys are conducted (at 23 nearfield stations). The most recent sediment contaminant monitoring and hard-bottom surveys were conducted in 2017. Sediment contaminant monitoring in 2017 continued to show no indication that toxic contaminants from the wastewater discharge are accumulating in depositional areas surrounding the outfall (Nestler et al. 2018). Monitoring results for 2017 also indicated that hard-bottom benthic communities near the outfall have not changed substantially during the post-diversion period as compared to the baseline period (Nestler et al. 2018).

This report summarizes key findings from the 2019 benthic surveys, with a focus on the most noteworthy observations relevant to understanding the potential effects of the discharge on the offshore benthic environment. Results of 2019 benthic monitoring were presented at MWRA's Annual Technical Workshop on April 24, 2020. This report builds on the presentations and discussions at that meeting.

2 METHODS

Methods used to collect, analyze, and evaluate all sample types remain largely consistent with those reported for previous monitoring years (Rutecki et al. 2019, Maciolek et al. 2008). Detailed descriptions of the methods are contained in the Quality Assurance Project Plan (QAPP) for Benthic Monitoring 2017–2020 (Rutecki et al. 2017). A brief overview of methods, focused on information that is not included in the QAPP, is provided in Sections 2.1 to 2.3.

2.1 FIELD METHODS

Sediment and infauna sampling was conducted at 14 stations on August 1, 2019 (Figure 2-1). To aid in analyses of potential spatial patterns reported herein, these stations are grouped, based on distance from the discharge, into four "monitoring areas" within Massachusetts Bay[1]:

- Nearfield stations NF13, NF14, NF17, and NF24, located in close proximity (less than 2 km) to the offshore outfall
- Nearfield stations NF04, NF10, NF12, NF20, NF21, and NF22, located in Massachusetts Bay but farther than 2 km (and less than 5 km) from the offshore outfall
- Transition area station FF12, located between Boston Harbor and the offshore outfall (just less than 8 km from the offshore outfall)
- Farfield reference stations FF01A, FF04, and FF09, located in Massachusetts Bay but farther than 13 km from the offshore outfall

Sampling effort at these stations has varied somewhat during the monitoring program. In particular, from 2004-2010 some stations were sampled only during even years (NF22, FF04 and FF09), Stations NF17 and NF12 were sampled each year, and the remaining stations were sampled only during odd years.

Sampling at Station FF04 within the Stellwagen Bank National Marine Sanctuary was conducted in accordance with Research Permit SBNMS-2016-003-A1.

Soft-bottom stations were sampled for grain size composition, total organic carbon (TOC), and the sewage tracer *Clostridium perfringens*. Infauna samples were also collected using a 0.04-m^2 Ted Young-modified van Veen grab, and were rinsed with filtered seawater through a 300-µm-mesh sieve.

Sediment Profile Imaging (SPI) samples were collected in triplicate at 23 nearfield stations on August 4, 2019 (Figure 2-2).

[1] The current monitoring areas form a subset of stations that were sampled before 2011. For example, the transition area formerly included station FF12 and two others that are no longer sampled.

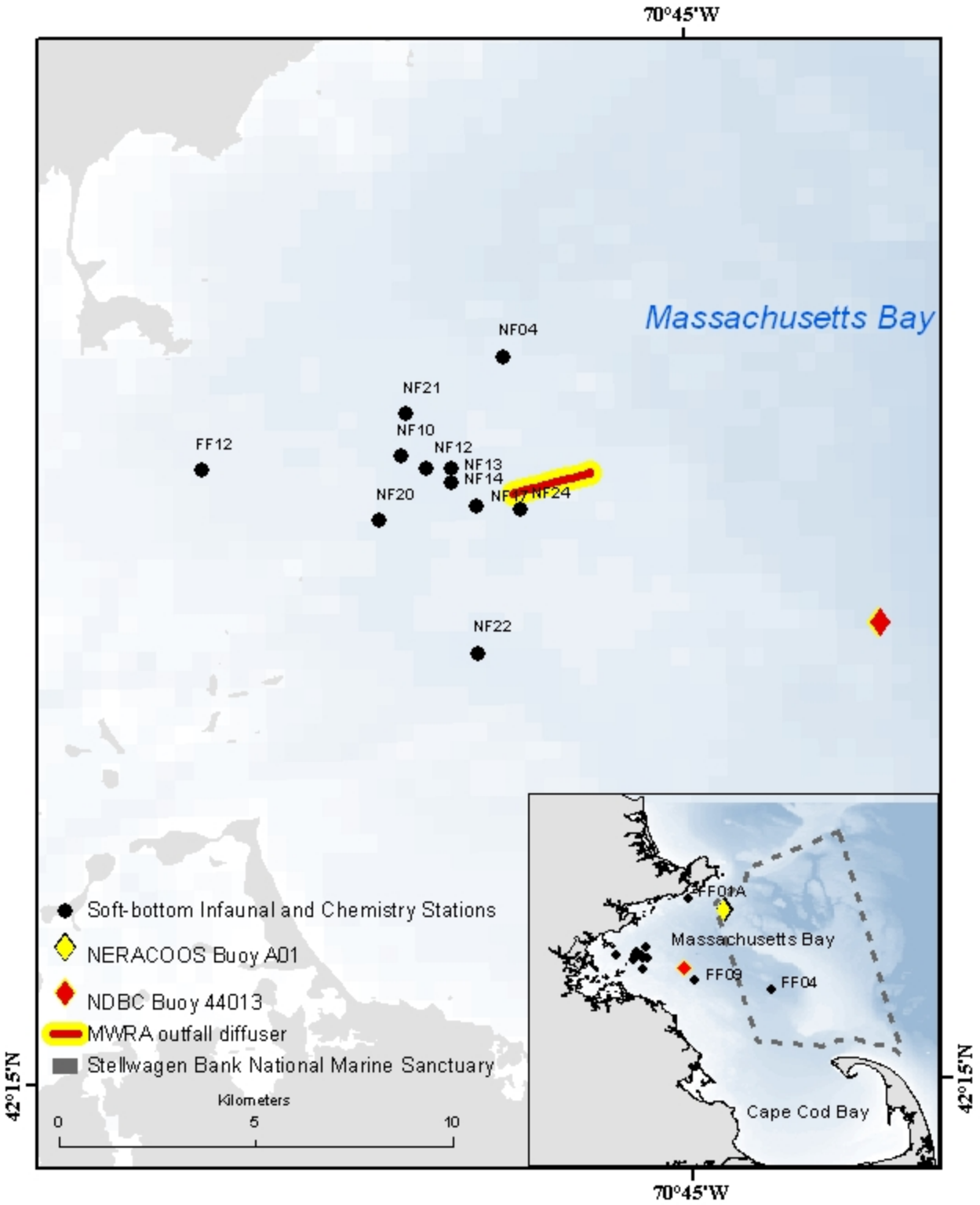

Figure 2-1. Locations of soft-bottom sampling stations for 2019.

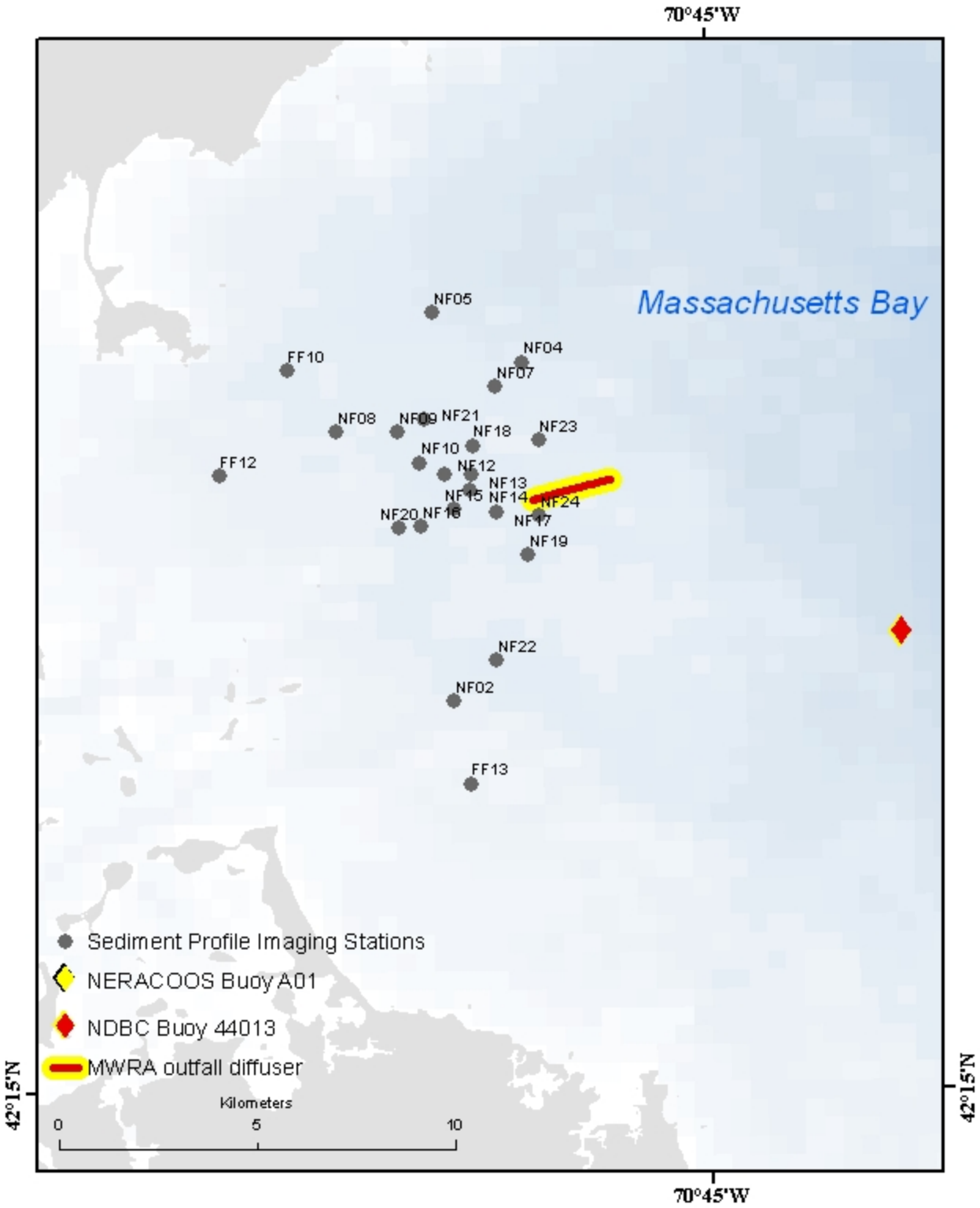

Figure 2-2. Locations of sediment profile imaging stations for 2019.

2.2 LABORATORY METHODS

All bacteriological, physical and chemical analyses were conducted by MWRA's DLS Laboratory following the procedures described in Constantino et al. (2014). All sample processing, including sorting, identification, and enumeration of infaunal organisms, was done following methods consistent with the QAPP (Rutecki et al. 2017).

2.3 DATA HANDLING, REDUCTION, AND ANALYSIS

All benthic data were extracted directly from the HOM database and imported into Excel. Data handling, reduction, graphical presentations and statistical analyses were performed as described in the QAPP (Rutecki et al. 2017) or by Maciolek et al. (2008).

Additional multivariate techniques were used to evaluate infaunal communities. Multivariate analyses were performed using PRIMER v6 (Plymouth Routines in Multivariate Ecological Research) software to examine spatial patterns in the overall similarity of benthic assemblages in the survey area (Clarke 1993, Warwick 1993, Clarke and Green 1988). These analyses included classification (cluster analysis) by hierarchical agglomerative clustering with group average linking and ordination by non-metric multidimensional scaling (MDS). Bray-Curtis similarity was used as the basis for both classification and ordination. Prior to analyses, infaunal abundance data were fourth-root transformed to ensure that all taxa, not just the numerical dominants, would contribute to similarity measures.

Cluster analysis produces a dendrogram that represents discrete groupings of samples along a scale of similarity. This representation is most useful when delineating among sites with distinct community structure. MDS ordination produces a plot or "map" in which the distance between samples represents their rank ordered similarities, with closer proximity in the plot representing higher similarity. Ordination provides a more useful representation of patterns in community structure when assemblages vary along a steady gradation of differences among sites. Stress provides a measure of adequacy of the representation of similarities in the MDS ordination plot (Clarke 1993). Stress levels less than 0.05 indicate an excellent representation of relative similarities among samples with no prospect of misinterpretation. Stress less than 0.1 corresponds to a good ordination with no real prospect of a misleading interpretation. Stress less than 0.2 still provides a potentially useful two-dimensional picture, while stress greater than 0.3 indicates that points on the plot are close to being arbitrarily placed. Together, cluster analysis and MDS ordination provide a highly informative representation of patterns of community-level similarity among samples. The "similarity profile test" (SIMPROF) was used to provide statistical support for the identification of faunal assemblages (i.e., selection of cluster groups). SIMPROF is a permutation test of the null hypothesis that the groups identified by cluster analysis (samples included under each node in the dendrogram) do not differ from each other in multivariate structure.

To help with assessment of spatial patterns, stations have been grouped into regions according to distance from the outfall. The monitoring areas include nearfield stations <2 km from the outfall, nearfield stations > 2 km from the outfall, a transition station, and farfield stations (see Section 2.1).

2.3.1 Data Reduction and Statistics for SPI Images

Details on parameters and analysis of SPI images can be found in Diaz et al. (2008). For this report, quantitative SPI parameters were averaged from the three replicate images. For categorical parameters the median value of the three replicate images was assigned to a station.

Since the selection of station locations in the nearfield was non-random, fixed-effect nominal logistic regression models were used to analyze patterns in categorical data (Agresti 1990). For continuous variables, the best fit of a suite of general linear models, either linear, exponential, second order polynomial, logarithmic, or power, were used to assess relationships between quantitative parameters (Draper and Smith 1998). Relationships between parameters were considered significant at alpha probability 0.05. Relationships between parameters were considered trends if alpha probability was between >0.05 and 0.10. All statistical tests were conducted with the statistical package R version 3.6.2 (2019-12-12) (The R Foundation for Statistical Computing at: https://www.r-project.org/foundation/).

3 RESULTS AND DISCUSSION

3.1 SEDIMENT CONDITIONS

3.1.1 *Clostridium perfringens*, Grain Size, and Total Organic Carbon

Sediment conditions were characterized by three parameters measured during 2019 at each of the 14 sampling stations: (1) *Clostridium perfringens*, (2) grain size (gravel, sand, silt, and clay), and (3) total organic carbon (Table 3-1).

Spores of the anaerobic bacterium *Clostridium perfringens* (reported as colony forming units per gram dry weight, normalized to percent fines) provide a sensitive tracer of effluent solids. A sharp increase *C. perfringens* concentrations at sites within two kilometers from the diffuser occurred coincident with diversion of effluent to the offshore outfall (Figure 3-1). *C. perfringens* concentrations have declined or remained comparable to the baseline at all other monitoring locations during the post-diversion period. Maciolek et al. (2007, 2008) confirmed that concentrations of *C. perfringens* were significantly higher at stations close to the outfall in 2006 and 2007 compared to pre-diversion concentrations and consistent with an impact of the outfall discharge. *C. perfringens* counts in samples collected during 2019 were modestly higher than the previous year at all locations, although counts increased only slightly at areas that are more than two kilometers from the outfall (Figure 3-1). This may be a result of year-year variability. As in past years during the post-diversion period, *C. perfringens* concentrations during 2019 continued to indicate a footprint of the effluent plume at sites closest to the discharge. Normalized *C. perfringens* spore counts in samples collected in 2019 were highest at station NF13 located within two kilometers of the outfall (Table 3-1, Figure 3-2).

Sediment texture in 2019 varied considerably among the 14 stations, ranging from almost entirely sand (e.g., NF17, NF13, and NF04) to predominantly silt and clay (i.e., FF04), with most stations having mixed sediments (Figure 3-3). Sediment texture has remained generally consistent over time, with relatively small year-to-year changes in the percent fine sediments at most stations (Figure 3-4). Annual variability in sediment texture at the Massachusetts Bay stations has typically been associated with strong storms. Sediment transport at water depths less than 50 meters near the outfall site in Massachusetts Bay occurs largely as a result of wave-driven currents during strong northeast storms (Bothner et al. 2002).

Concentrations of TOC in 2019 remained similar to values reported in prior years at most stations (Figure 3-5). Higher TOC values were generally associated with higher percent fines (compare Figures 3-4 and 3-5). To further assess spatial patterns in TOC concentrations while accounting for the association between TOC and percent fine sediments, TOC values were normalized to percent fines (Figure 3-6). Although there was a sharp increase in TOC at NF17 in 2019, TOC at NF17 in 2020 were more similar to most previous years.

C. perfringens counts continue to provide evidence of effluent solids depositing near the outfall. There is no indication, however, that the wastewater discharge has resulted in changes to the sediment grain size composition at the Massachusetts Bay sampling stations, and there is no indication of organic enrichment.

Overall, TOC concentrations remain comparable to, or lower than, values reported during the baseline period, even at sites closest to the outfall (Figures 3-7 and 3-8).

Table 3-1. Monitoring results for sediment condition parameters in 2019.

Monitoring Area	Station	*Clostridium perfringens* (cfu/g dry/%fines)	Total Organic Carbon (%)	Gravel (%)	Sand (%)	Silt (%)	Clay (%)	Percent Fines (Silt + Clay)
Transition Area	**FF12**	35.5	0.42	3.2	69.3	21.5	6.1	27.6
Nearfield (<2 km from outfall)	**NF13**	361.6	0.13	3.1	93.3	1.4	2.1	3.5
	NF14	132.9	0.57	23.3	65.8	6.9	4.0	10.9
	NF17	221.0	0.14	0.0	98.2	0.1	1.7	1.8
	NF24	143.1	0.17	0.0	93.2	4.5	2.4	6.9
Nearfield (>2 km from outfall)	**NF04**	131.1	0.16	1.0	94.3	3.1	1.7	4.7
	NF10	17.3	0.65	1.9	64.1	24.4	9.6	34.1
	NF12	16.0	1.16	0.0	33.6	52.7	13.7	66.4
	NF20	51.8	0.63	25.7	59.6	10.1	4.6	14.7
	NF21	25.9	1.08	0.0	46.2	43.3	10.5	53.8
	NF22	28.2	0.90	0.0	60.3	30.1	9.6	39.7
Farfield	**FF01A**	98.8	0.28	1.6	87.7	8.4	2.3	10.6
	FF04	4.0	2.23	0.0	10.3	58.7	31.0	89.8
	FF09	6.3	0.37	0.0	86.0	6.4	7.7	14.0

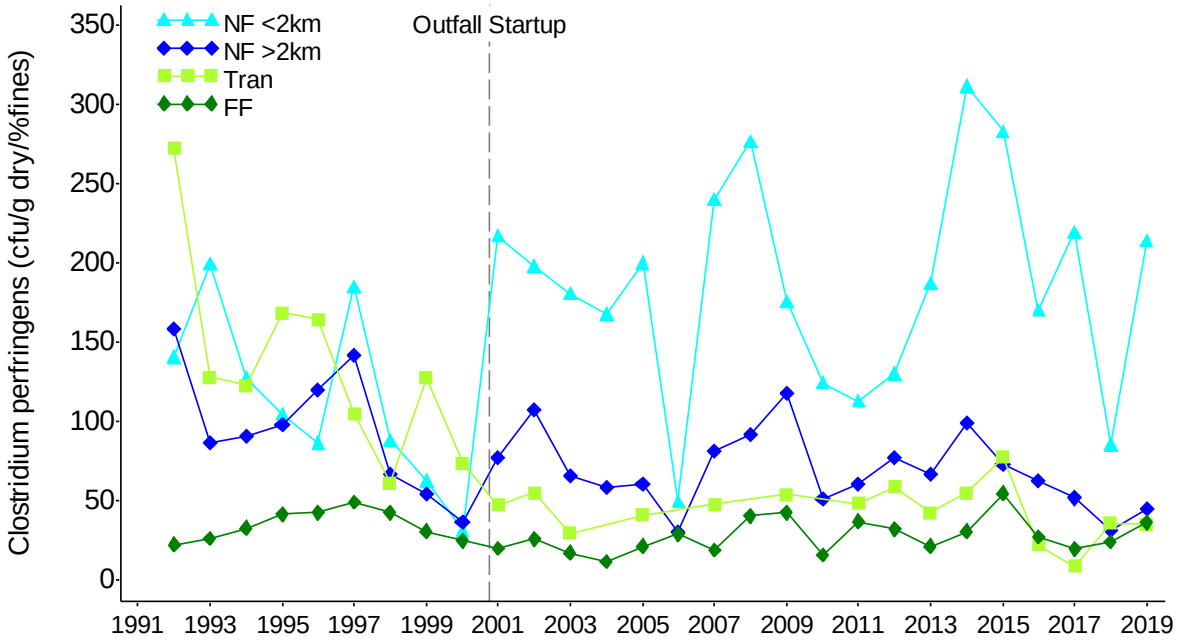

Figure 3-1. Mean concentrations of *Clostridium perfringens* in four areas of Massachusetts Bay, 1992 to 2019. Tran=Transition area; NF<2km=nearfield, less than two kilometers from the outfall; NF>2km=nearfield, more than two kilometers from the outfall; FF=farfield.

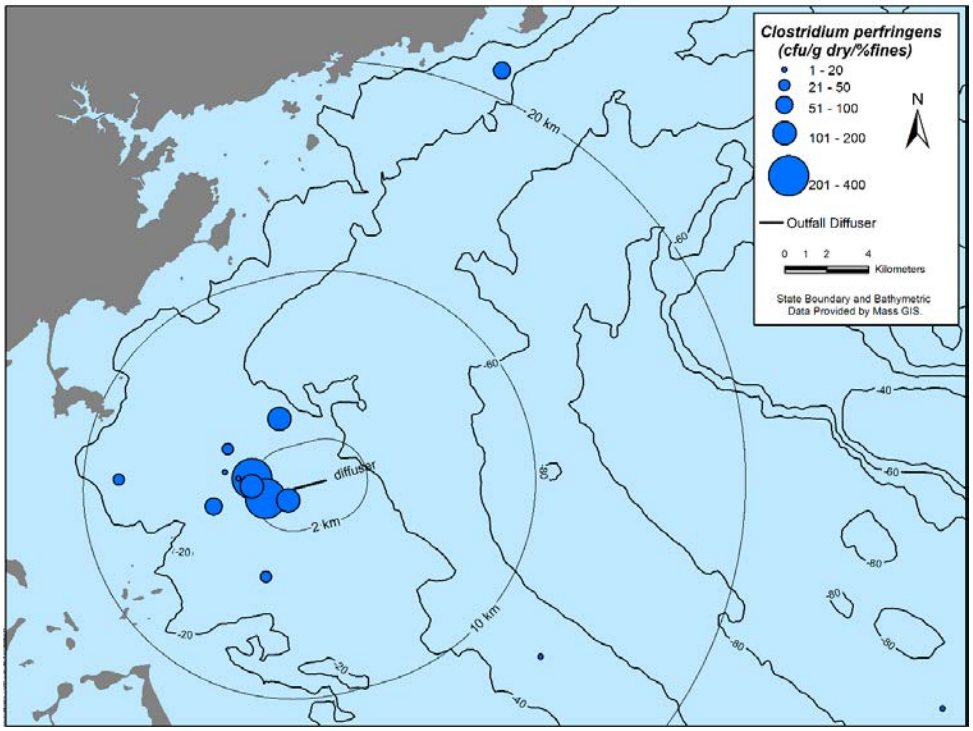

Figure 3-2. Monitoring results for *Clostridium perfringens* in 2019.

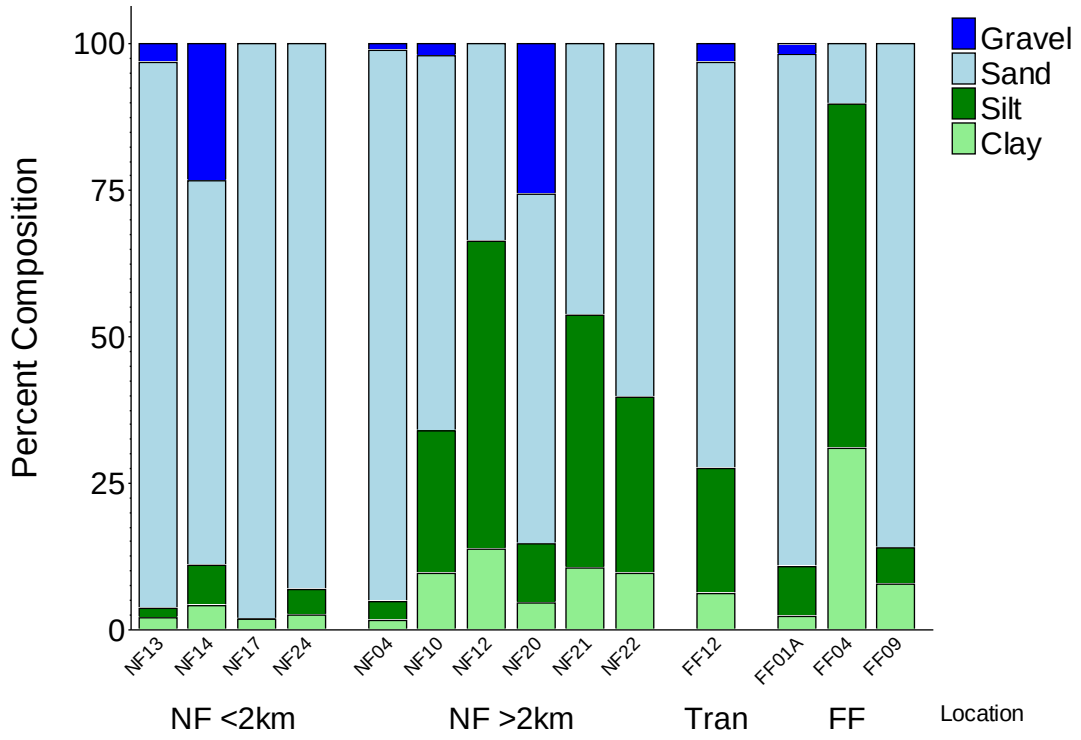

Figure 3-3. Monitoring results for sediment grain size in 2019.

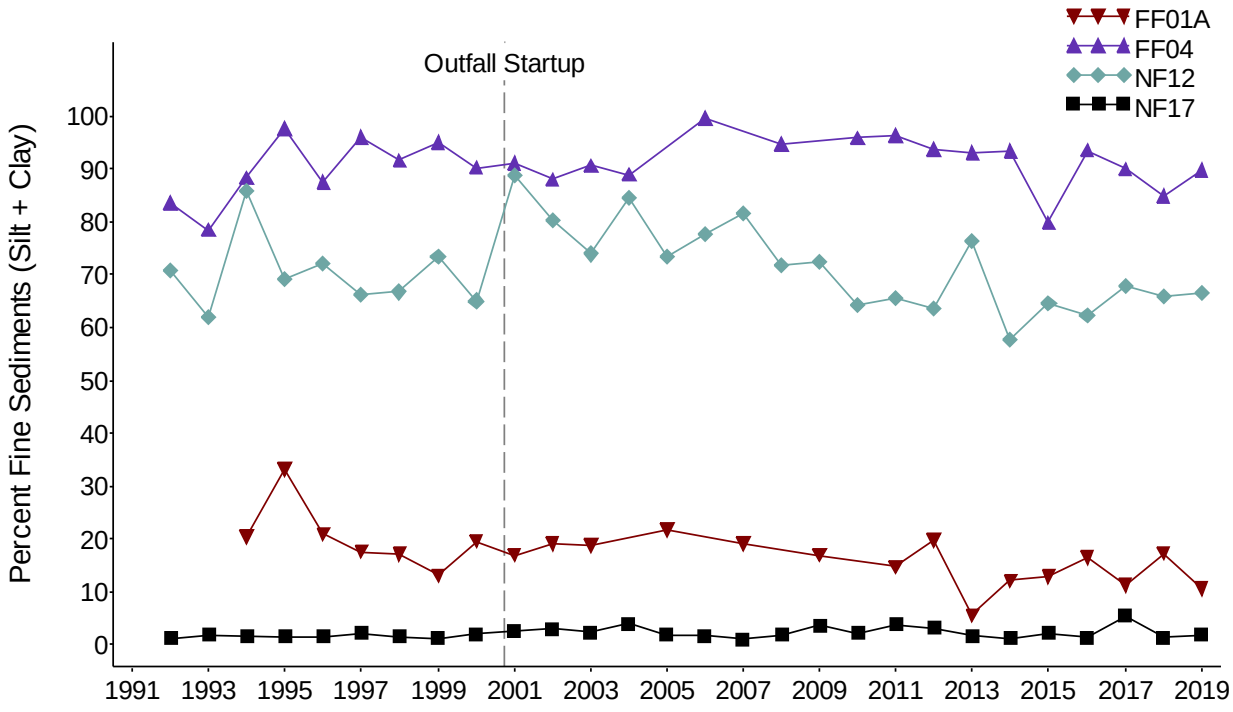

Figure 3-4. Mean percent fine sediments at FF01A, FF04, NF12 and NF17; 1992 to 2019.

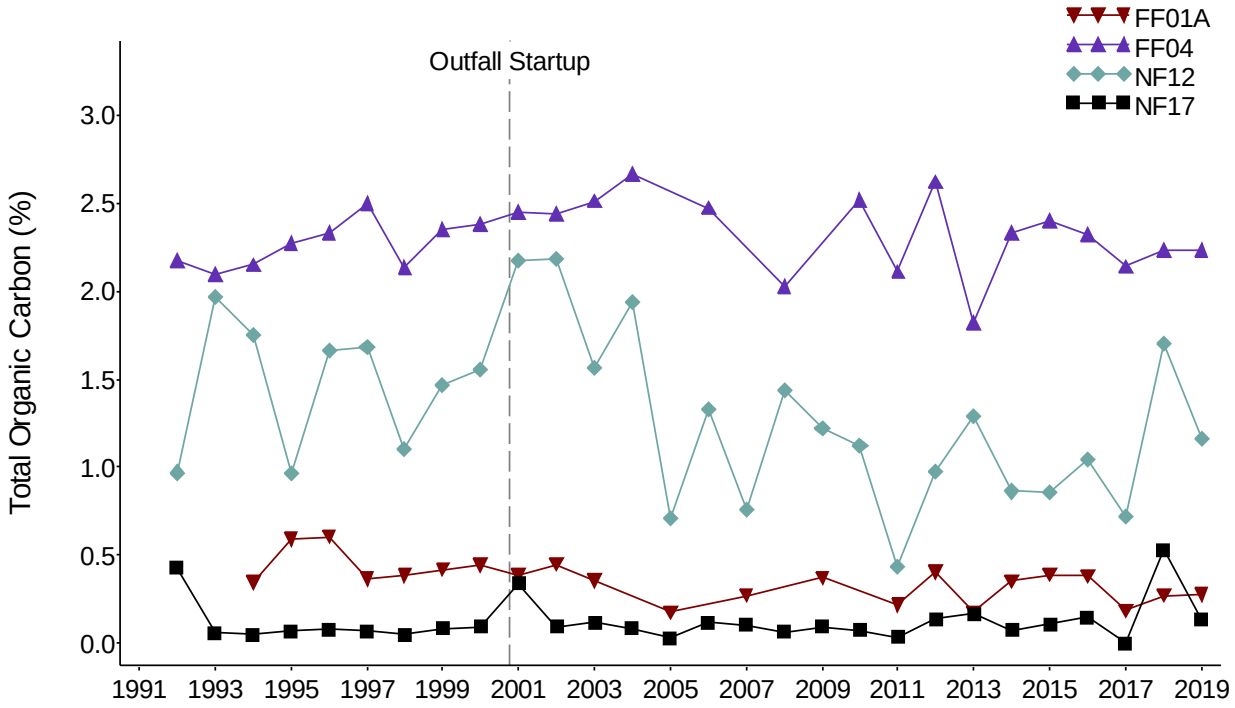

Figure 3-5. Mean concentrations of TOC at four stations in Massachusetts Bay, 1992 to 2019.

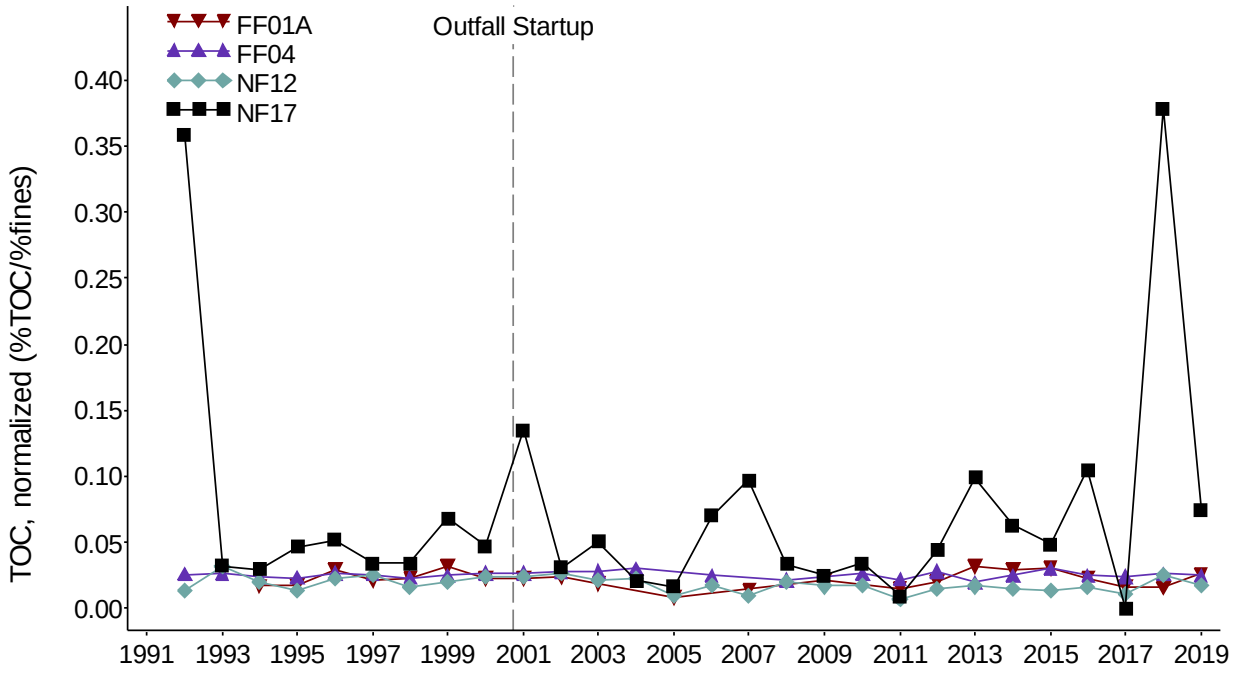

Figure 3-6. Normalized mean concentrations of TOC at four stations in Massachusetts Bay, 1992 to 2019.

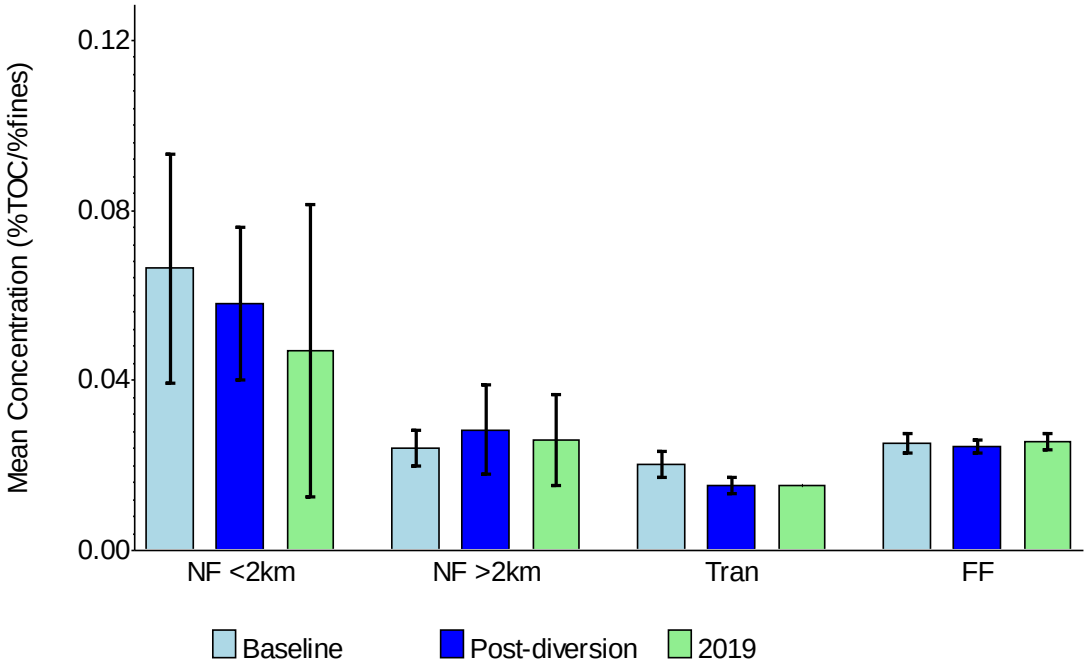

Figure 3-7. Normalized mean (with 95% confidence intervals) concentrations of TOC at four areas in Massachusetts Bay during the baseline (1992 to 2000) and post-diversion (2001 to 2018) periods compared to 2019. Tran=Transition area; NF<2km=nearfield, less than two kilometers from the outfall; NF>2km=nearfield, more than two kilometers from the outfall; FF=farfield.

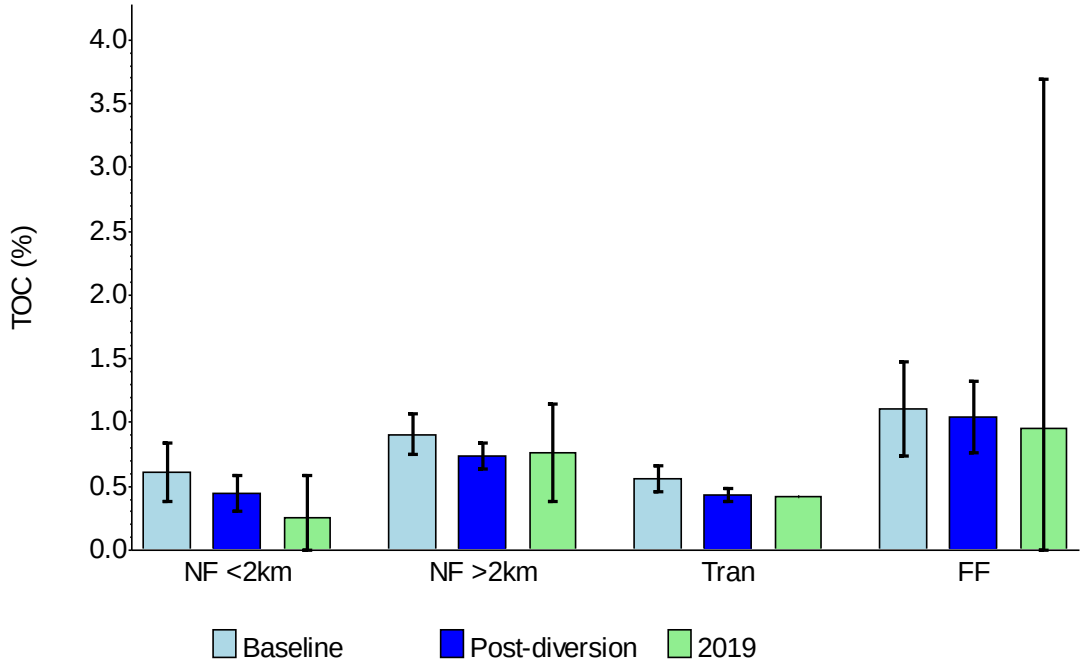

Figure 3-8. Mean (with 95% confidence intervals) concentrations of TOC at four areas in Massachusetts Bay during the baseline (1992-2000) and post-diversion (2001 to 2018) compared to 2019.

3.2 BENTHIC INFAUNA

3.2.1 Community Parameters

A total of 26,614 infaunal organisms were counted from the 14 samples in 2019. Organisms were classified into 213 discrete taxa; 185 of those taxa were species-level identifications. The abundance values reported herein reflect the total counts from both species and higher taxonomic groups, while all diversity measures and multivariate analyses are based on the species-level identifications only (Table 3-2).

Total abundance values in 2019 were lower than the 2018 values at all areas in Massachusetts Bay except the nearfield stations located within 2 kilometers from the discharge (Figure 3-9). Abundance at Station FF12 (the only station in the "Transition Area"), remained higher than means for the other areas in the Bay for a sixth consecutive year (Figure 3-9) although higher abundances were observed at some individual nearfield stations such as NF24 (Table 3-2). The numbers of species per sample in 2019 were slightly higher than in 2018 at all locations, and mean values remained relatively similar across all areas of the Bay (Figure 3-10). There were no Contingency Plan threshold exceedances for any infaunal diversity measures in 2019 (Table 3-3). Shannon-Wiener Diversity (H') and Pielou's Evenness (J') values at the nearfield stations were higher in 2019 compared to the previous year, but similar to values reported during other recent years (Figures 3-11 and 3-12).

Spatial and temporal patterns of abundance, species richness, species diversity and evenness generally support the conclusion that there is no evidence of negative impacts caused by operation of the offshore outfall.

Table 3-2. Monitoring results for infaunal community parameters in 2019.

Monitoring Area	Station	Total Abundance (per grab)	Number of Species (per grab)	Log-series alpha	Shannon-Wiener Diversity (H′)	Pielou's Evenness (J')
Transition Area	**FF12**	2835	60	10.77	3.40	0.58
Nearfield (<2 km from outfall)	**NF13**	1270	72	16.72	4.21	0.68
	NF14	1201	66	15.08	3.81	0.63
	NF17	876	45	10.11	3.46	0.63
	NF24	3425	71	12.68	3.61	0.59
Nearfield (>2 km from outfall)	**NF04**	1161	63	14.51	4.11	0.69
	NF10	2694	69	12.97	4.00	0.65
	NF12	1596	58	11.82	4.01	0.68
	NF20	2615	61	11.20	3.54	0.60
	NF21	2847	73	13.71	4.40	0.71
	NF22	2728	67	12.46	4.19	0.69
Farfield	**FF01A**	1441	58	12.22	3.76	0.64
	FF04	749	36	7.89	3.52	0.68
	FF09	1176	82	20.38	4.61	0.73

Table 3-3. Infaunal monitoring threshold results, August 2019 samples.

Parameter	Thresholds*		Result	Exceedance?
	Value	Limit		
Total species	42.99	Low	64.09	No
Log-series Alpha	9.42	Low	12.91	No
Shannon-Weiner H′	3.37	Low	3.88	No
Pielou's J'	0.57	Low	0.65	No
Apparent RPD	1.18	Low	4.85	No
Percent opportunists	10% (Caution)	High	0.28	No
Percent opportunists	25% (Warning)	High	0.28	No

*Threshold exceedances occur when current year results are below threshold values for a "low" limit or above the values for a "high" limit for a given parameter.

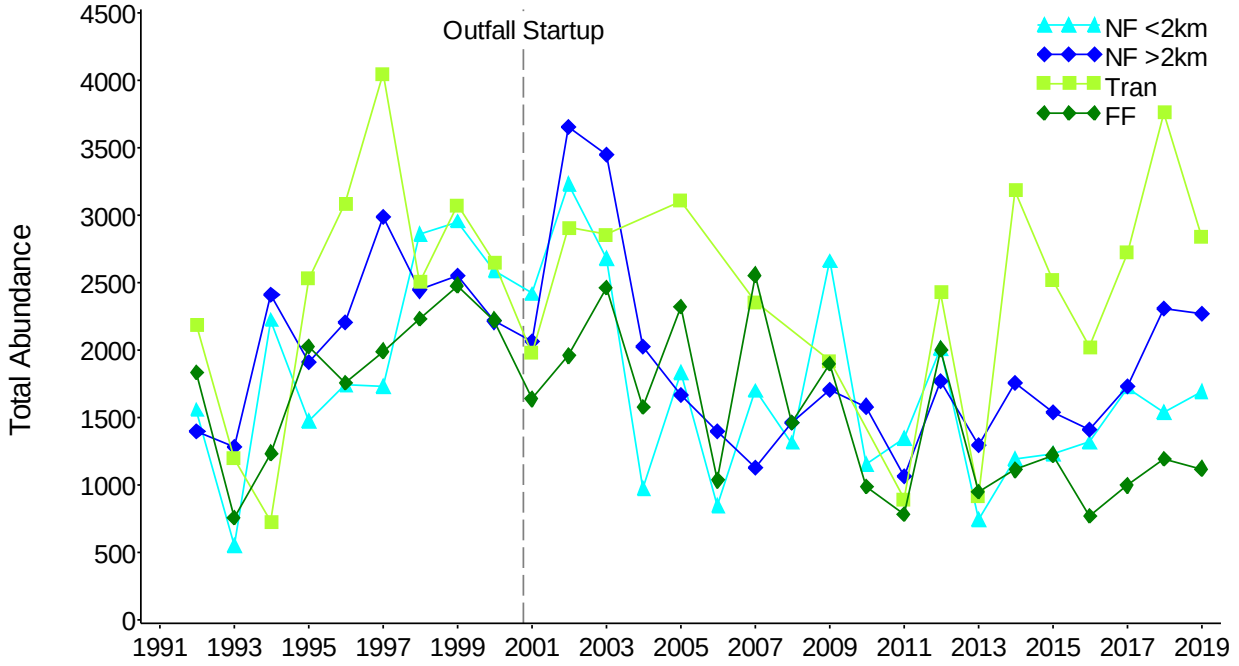

Figure 3-9. Mean infaunal abundance per sample at four areas of Massachusetts Bay, 1992 to 2019. Tran=Transition area; NF<2km=nearfield, less than two kilometers from the outfall; NF>2km=nearfield, more than two kilometers from the outfall; FF=farfield.

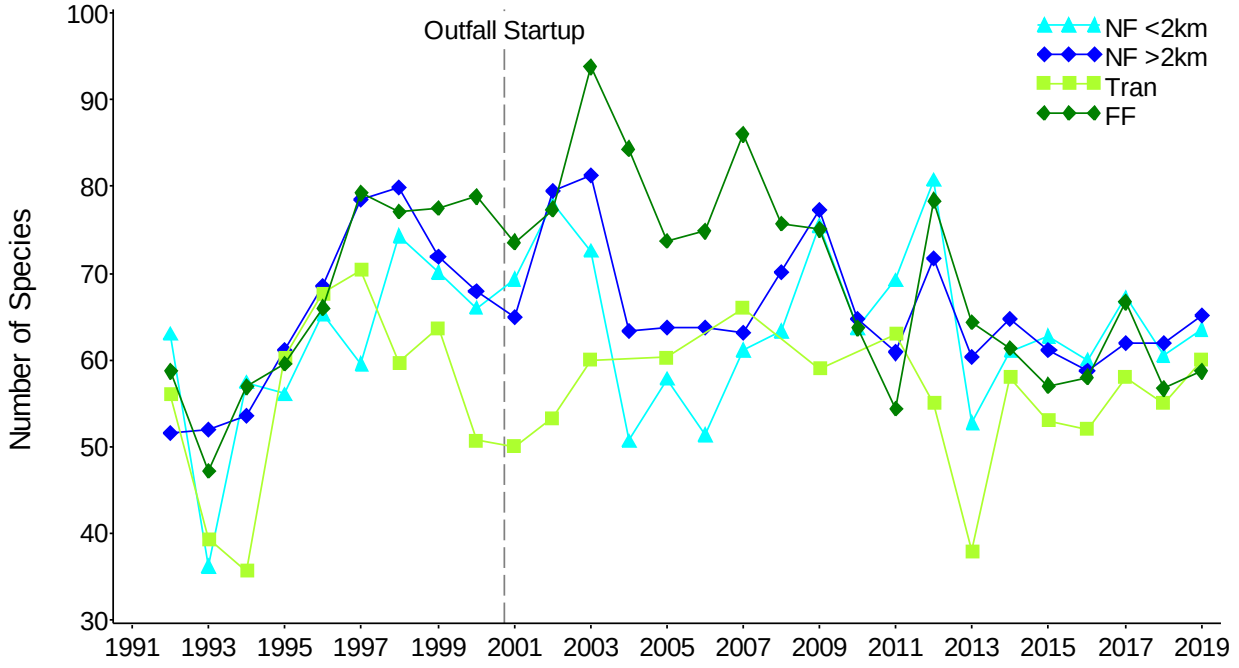

Figure 3-10. Mean number of species per sample at four areas of Massachusetts Bay, 1992 to 2019. Tran=Transition area; NF<2km=nearfield, less than two kilometers from the outfall; NF>2km=nearfield, more than two kilometers from the outfall; FF=farfield.

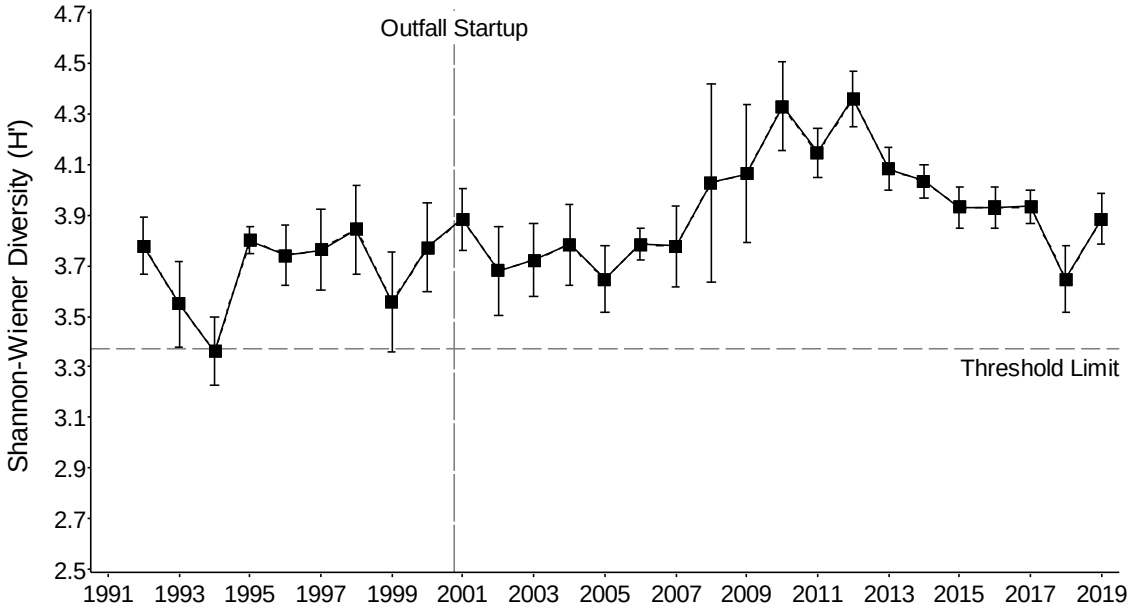

Figure 3-11. Mean (and 95% confidence intervals) Shannon-Wiener Diversity (H′) at nearfield stations in comparison to threshold limit, 1992 to 2019. The nearfield annual means and associated threshold limit are both based on the list of stations sampled following the 2010 revision to the Ambient Monitoring Plan (MWRA 2010).

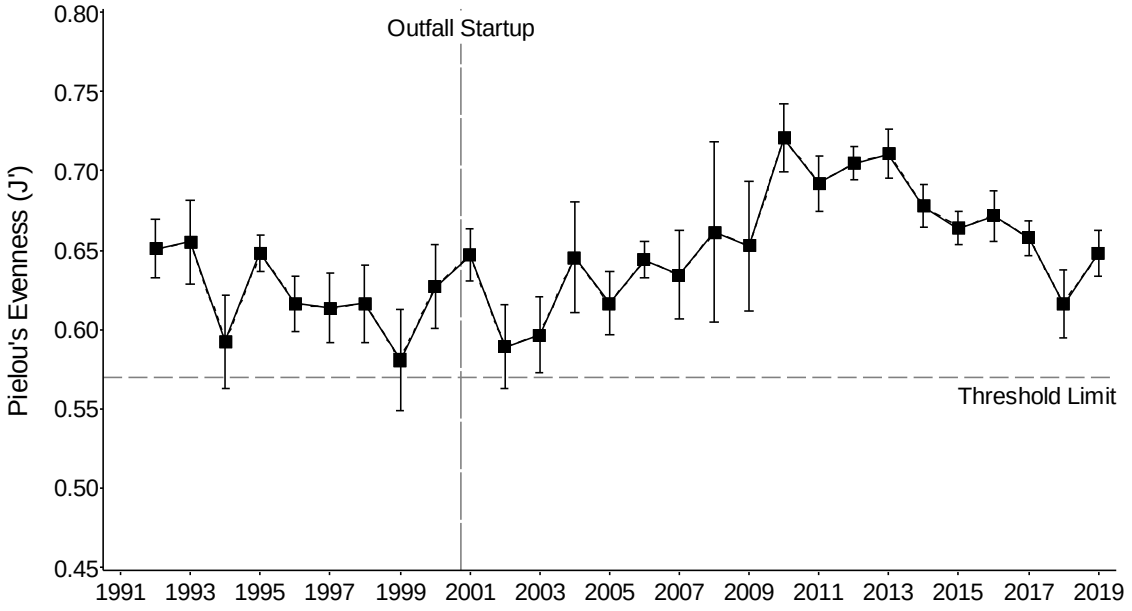

Figure 3-12. Mean (and 95% confidence intervals) Pielou's Evenness (J′) at nearfield stations in comparison to threshold limit, 1992 to 2019. The nearfield annual means and associated threshold limit are both based on the list of stations sampled following the 2010 revision to the Ambient Monitoring Plan (MWRA 2010).

3.2.2 Infaunal Assemblages

Multivariate analyses based on Bray-Curtis Similarity were used to assess spatial patterns in the faunal assemblages at the Massachusetts Bay sampling stations. Two main assemblages (Groups I and II) and an outlier assemblage (Group III) were identified in a cluster analysis of the 14 samples from 2019 (Figure 3-13). The groups were distinguished based on species composition and the relative abundances of each taxon in the samples. Clear differences in the mean abundances of dominant taxa were identified. Abundances at the stations included in Groups I and III were generally two to three times lower than Group II (compare Figure 3-13 with Table 3-2). Although arthropods were dominant at Station NF17, most assemblages were dominated by polychaetes (Table 3-4). Several species were dominant only in Group I (e.g., *Crassicorophium crassiorne, Pseudunciola obliquua*, *Molgula manhattensis* and *Chiridotea tuftsi*), while others were more prevalent in Group II (e.g., *Ennucula delphinodonta, Owenia artifex,* and cirratulids in the genus *Kirkegaardia*) or in Group III (e.g., *Paramphinome jeffreysii* and *Cossura longocirrata*). Group I consisted of two subgroups and was composed of three nearfield stations (Group IA: Stations NF04 and NF13; NF17). The Group II assemblage included three subgroups (Group IIA: Stations FF01A, FF09; Group IIB: Stations NF14, NF20, and FF12; and Group IIC: Stations NF24, NF10, NF22, NF21, and NF12) that could be differentiated by species composition and total abundance. The relatively deep Station FF04 was characterized by low abundances and species richness. The outlier assemblage that was found at this station was labeled as Group III. Dominant species at Station FF04, including *Levinsenia gracilis, Cossura longocirrata,* and *Chaetozone anasimus*, are characteristic of the soft sediment community observed throughout Stellwagen Basin (e.g., Maciolek et al. 2008).

Both main assemblages (Groups I and II) occurred at one or more each of the four stations within two kilometers of the discharge as well as at stations more than two kilometers from the discharge (Figure 3-14). Thus, stations closest to the discharge were not characterized by a unique faunal assemblage reflecting effluent impacts. Comparisons of faunal distribution to habitat conditions indicated that patterns in the distribution of faunal assemblages follow differences in habitat types at the sampling stations and are associated with the sediment types at the sampling stations (Figure 3-15) and with station depth (not shown).

Patterns identified in these analyses were highly consistent with previous years. No evidence of impacts from the offshore outfall on infaunal communities in Massachusetts Bay was found.

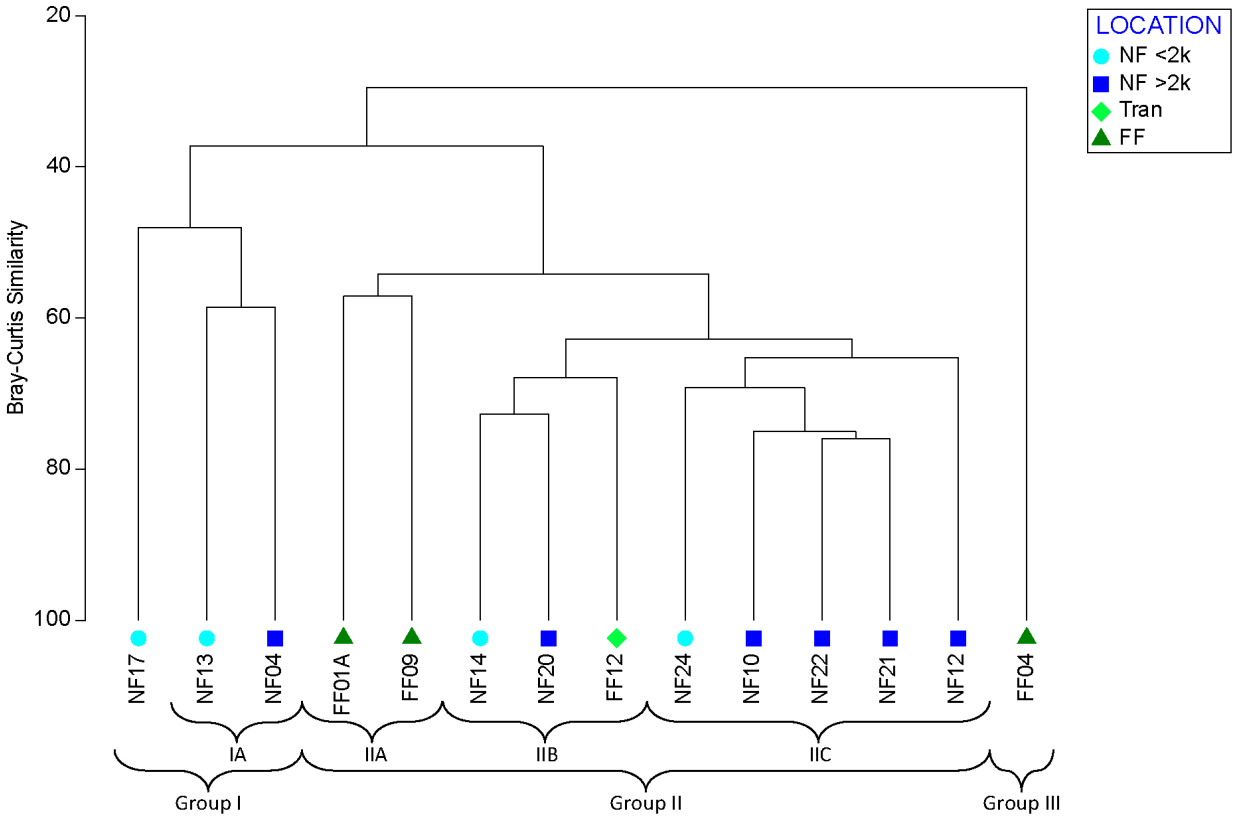

Figure 3-13. Results of cluster analysis of the 2019 infauna samples.

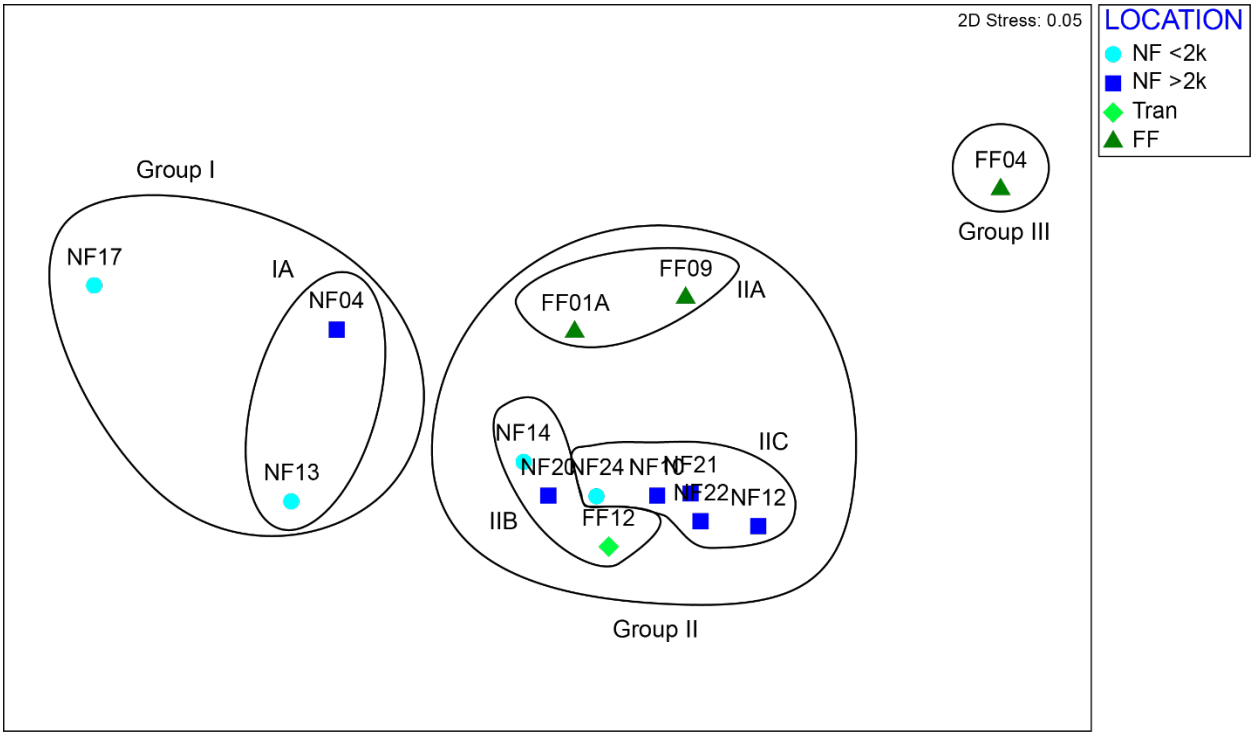

Figure 3-14. Results of a MDS ordination of the 2019 infauna samples from Massachusetts Bay showing distance from the outfall.

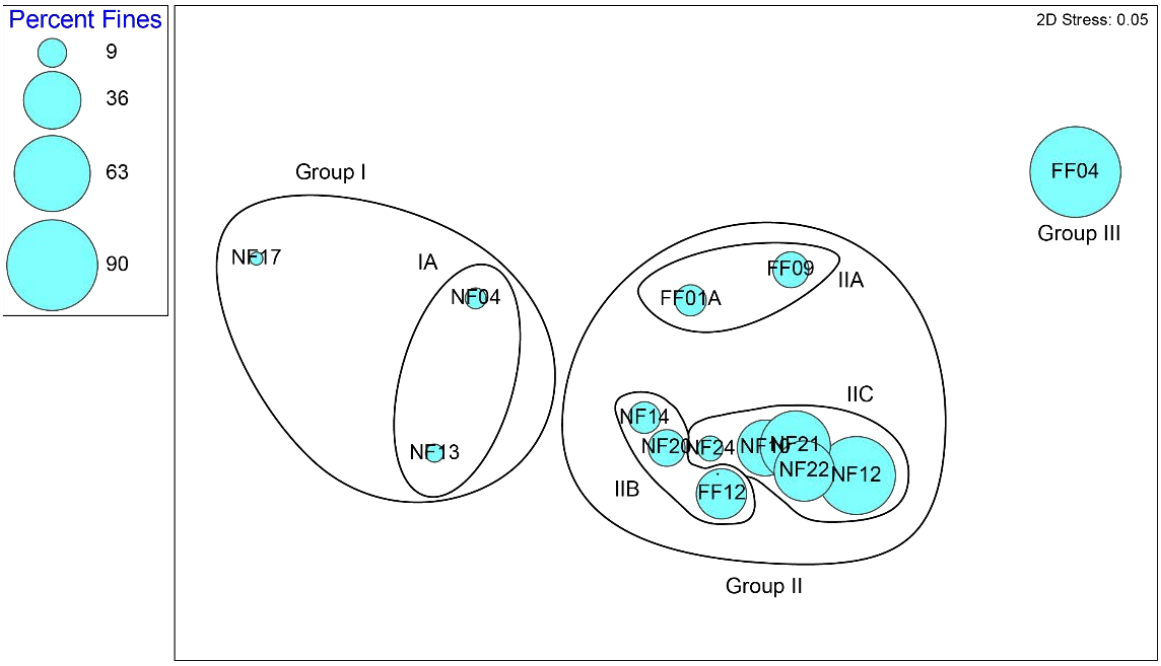

Figure 3-15. Percent fine sediments superimposed on the MDS ordination plot of the 2019 infauna samples. Each point on the plot represents one of the 14 samples; similarity of species composition is indicated by proximity of points on the plot. Faunal assemblages (Groups I-II, and sub-groups) identified by cluster analysis are circled on the plot. The ordination and cluster analysis are both based on Bray-Curtis Similarity.

Table 3-4. Abundance (mean # per grab) of numerically dominant taxa (10 most abundant per group) composing infaunal assemblages identified by cluster analysis of the 2019 samples.

Family	Species	Group I		Group II			Group III
		NF17	IA	IIA	IIB	IIC	FF04
Nemertea							
	Nemertea sp. 12	-	0.5	14.8	8.3	11.0	23.0
Mollusca (Bivalvia)							
Mytilidae	*Crenella decussata*	3.0	-	0.4	0.7	38.0	-
Nuculidae	*Ennucula delphinodonta*	-	9.5	9.6	22.3	156.0	1.0
Annelida (Polychaeta)							
Ampharetidae	*Anobothrus gracilis*	-	1.0	2.6	2.0	60.0	36.0
Amphinomidae	*Paramphinome jeffreysii*	-	-	-	-	-	56.0
Capitellidae	*Mediomastus californiensis*	-	4.0	296.4	131.7	23.0	16.0
Cirratulidae	*Chaetozone anasimus*	1.0	24.5	-	0.3	1.0	135.0
	Kirkegaardia baptisteae	-	6.0	168.2	135.3	15.5	-
	Kirkegaardia hampsoni	-	0.5	70.6	85.7	14.5	-
	Tharyx acutus	1.0	112.5	296.6	207.3	26.0	-
Cossuridae	*Cossura longocirrata*	-	-	8.4	0.3	2.0	86.0
Lumbrineridae	*Ninoe nigripes*	-	2.0	94.2	50.7	33.5	14.0
	Scoletoma hebes	-	1.0	22.6	81.7	-	-
Maldanidae	*Clymenella torquata*	-	28.5	18.8	6.0	2.5	-
Orbiniidae	*Leitoscoloplos acutus*	-	1.0	112.8	13.7	5.5	9.0
Oweniidae	*Owenia artifex*	-	2.5	15.2	0.3	230.5	-
Paraonidae	*Aricidea catherinae*	7.0	176.0	256.2	583.7	26.0	-
	Aricidea quadrilobata	-	-	9.6	0.3	27.0	46.0
	Levinsenia gracilis	-	-	176.8	82.3	97.0	216.0
Phyllodocidae	*Phyllodoce mucosa*	28.0	40.5	35.8	23.3	9.0	-
Polygordiidae	*Polygordius jouinae*	46.0	72.0	7.6	15.3	28.5	-
Sabellidae	*Euchone incolor*	-	2.0	67.0	19.3	31.5	21.0
Spionidae	*Prionospio steenstrupi*	4.0	23.5	468.8	478.3	171.0	9.0
	Spio thulini	8.0	25.5	2.0	16.3	28.0	-
	Spiophanes bombyx	32.0	32.5	75.4	47.3	16.0	-
Syllidae	*Exogone hebes*	32.0	211.0	24.4	40.3	5.5	-
Arthropoda (Amphipoda)							
Corophiidae	*Crassicorophium crassicorne*	278.0	130.0	-	1.3	-	-
Phoxocephalidae	*Rhepoxynius hudsoni*	11.0	6.5	-	-	-	-
Unciolidae	*Pseudunciola obliquua*	204.0	-	-	-	-	-
Arthropoda (Isopoda)							
Chaetiliidae	*Chiridotea tuftsi*	35.0	10.0	-	-	-	-
Arthropoda (Tanaidacea)							
Nototanaidae	*Tanaissus psammophilus*	21.0	9.5	-	-	0.5	-
Chordata (Urochordata)							
Molgulidae	*Molgula manhattensis*	47.0	4.0	-	-	1.0	-

3.3 SEDIMENT PROFILE IMAGING

General Benthic Habitat Conditions

There continues to be no evidence of an outfall effect on infaunal benthic habitat quality based on sediment profile imaging (SPI) data for 2019. Comparing baseline habitat conditions (1992 to 2000) with post-baseline outfall operation conditions (2001 to 2019) found that there has not been any changes in benthic habitat quality attributable to outfall operation. Changes that have occurred appeared to be regional and not associated with outfall operation.

Annual comparisons in apparent color redox-potential discontinuity (aRPD) layer depth, an MWRA threshold parameter, between the baseline period and the 19-year outfall operational period have consistently shown the aRPD layer depth to have remained the same or significantly increased though time (Figure 3-16). On average, aRPD layer depths increased 0.13 cm per year from 1992 to 2019 (linear regression, $R^2 = 0.77$, $p = <0.001$), with 2019 being among the years with deepest aRPD layers (Table 3-5).

Being among the highest annual averages for post outfall monitoring, the grand mean aRPD layer depth in 2019 did not exceed the threshold of a 50% decrease from the baseline conditions (Figure 3-16). If only measured values are considered the thickness of the aRPD for 2019 would be 4.8 cm (SD = 0.8 cm, 15 stations in mean). At 8 of the 23 stations, the aRPD was deeper than prism penetration due to coarse grain size and high sediment compaction that limited prism penetration. From the start of SPI monitoring in 1992 to 2000, the baseline period, the thickness of the annual mean aRPD layer averaged 2.2 cm (Table 3-5).

The deepening of the aRPD layer through time along with an increase in the Organism Sediment Index (OSI, a measure of benthic habitat quality, Rhoads and Germano 1986) indicated the presence of high quality benthic habitat in the nearfield (Figure 3-16). The OSI fell below 6 (indicating poor benthic habitat quality, Rhoads and Germano 1986) twice over the monitoring period, in 1997 and gain in 2003 (Figure 3-16). Overall, the OSI increased by 0.1 unit per year (linear regression, $R^2 = 0.60$, $p = <0.001$). Community structure and high diversity of benthos also confirmed the presence of high quality benthic habitat (Rutecki et al. 2019). Had outfall operation degraded benthic habitat quality both aRPD layer depth and diversity would have declined, as observed at other ocean outfalls (Puente and Diaz 2015).

These findings support MWRA's discussions with recommendation to regulatory agencies and OMSAP in 2019 that the SPI study in Massachusetts Bay had answered relevant monitoring questions fully and could be ended. OMSAP endorsed this recommendation at their October 3, 2019 meeting, and MWRA proposed this monitoring change to take effect during summer, 2020.

Benthic Habitat Patterns

The nearfield benthic monitoring program represents a 28-year (1992-2019) series of annual snapshots intended to document pre- and post- outfall operation conditions on benthic habitats and communities. We found SPI, benthic community, and sedimentary parameters to be variable and continuously changing throughout the monitoring period (Figures 3-9 and 3-11; Figures 3-16 and 3-17). Some of the change was systematic and some stochastic. In all cases the changes were complex, asynchronous, and driven by a combination of factors acting at broad regional and/or temporal scales. Benthic habitats and communities did not show evidence of an outfall effect as most of the trends observed in the data appeared driven by a complex mix of factors acting at scales larger than the nearfield area.

The likely forcing factors acting in the nearfield, both on pelagic and benthic ecosystems would be a combination of anthropogenic, oceanographic, and climatic factors (Figure 3-18). The obvious anthropogenic factors would be the outfall and other sources of coastal eutrophication. The impacts of these two factors would be mediated by broad regional circulation patterns (Signell et al 2000). These in turn would be subject to long-term effects of climate change, which will alter sea level, storminess, wind and wave energy, temperature, and salinity (USGCRP 2017, Talke et al. 2018, Voorhies et al. 2018, Reguero et al. 2019, Werme et al. 2019).

Overall, the monitoring program supports the conclusion that the outfall appears to be a minor contributor to change in both pelagic and benthic (both soft and hard bottom) ecosystems outside of the immediate area of the outfall. Water-column monitoring in Massachusetts Bay found limited effects of the discharge at stations located in close proximity to the outfall (Libby et al. 2019, Werme et al. 2019). Infaunal monitoring found no effects from outfall operation beyond a localized increase in spores of *Clostridium perfringens* (also discussed in Section 3.1 of this report) (Rutecki et al. 2019). The hard bottom surveys did document increases in biomass and abundance of some epifaunal species (for example, the anemone *Metridium senile* and the hydroid *Tubularia* sp.) on and immediately around the outfall diffuser heads, but no effects farther away from the outfall (Maciolek et al. 2008, Nestler et al. 2018). Interestingly, hydroids and anemones also increased on diffuser heads during baseline monitoring before outfall start-up.

In general, monitoring data point to physical rather than biological processes as the driving factors in the nearfield, which lessens the chances of the outfall affecting the benthic environment (Werme et al. 2019). For ocean outfalls located in high energy regions, such as the MWRA nearfield, tidal or storm induced turbulence and currents are the primary factors controlling benthic impacts (Signell et al. 2000, Warner et al. 2008, Puente and Diaz 2015). Clover Point, British Colombia, Canada, is an example of a tidally dominated outfall (Chapman et al. 1996) and Mar del Plata City, Argentina, an example of storm dominated outfall (Elías et al. 2005). At both outfalls strong tidal and storm currents lessened outfall impacts on the benthos.

Climate through its effect on storminess has emerged as a principle driving factor of change for benthic ecosystems in many regions (Labrune et al. 2007, Voorhies et al. 2018, Foulquier et al. 2020). Storms and storm-induced sediment transport tend to be the primary controlling factors for benthic habitats and communities (Kröncke et al. 1998, Butman et al. 2008, Voorhies et al. 2018, Foulquier et al. 2020). Climate is also a likely factor for driving change in pelagic ecosystems (Turner et al. 2006, Fulweiler and Nixon 2009). For the nearfield area, on the western side of Massachusetts Bay, the number of winter-period storms (October to May prior to the August monitoring fieldwork) increased by 4% per decade from 1990-2018 and intensity of storms (estimated as integrated wave stress at 30 m depth) increased by 15% per decade (Rutecki et al. 2019). In terms of timing, five (2005, 2010, 2013, 2015, 2018) of the seven stormiest years occurred after the outfall went online in September 2000. Pre-outfall high storm years were 1993 and 1998 (Figure 3-19). The least stormy year from 1990 to 2018 was 2002, two years after the outfall went online, followed by 1999, 2009, 1995, and 2014.

In addition to storms, climate is likely driving changes in temperature and salinity. Temperature increased about half a degree centigrade per decade (+0.48 C) and salinity by about 0.17 psu per decade (Figure 3-20). It is also likely that climate interacts with other sources of coastal eutrophication effecting both nearfield pelagic and benthic conditions (Fulweiler and Nixon 2009).

Through time, there were systematic changes in benthic habitats over the entire nearfield driven largely by interactions of time, climate, and benthos. To assess changes across the environmental gradients found in the nearfield, we used annual averages for all 23 stations. Superimposed on these long-term trends was a high degree of year-to-year variation. There were significant trends in aRPD layer depth and the OSI, both of which increased through time (Figure 3-16). Estimated successional stage declined through time from a nearfield average of intermediate Stage II and equilibrium Stage III fauna, to Stage II tending to

pioneering Stage I (Figure 3-17). Total number of biogenic structures (the sum of infauna, burrows, and feeding voids) observed in SPI also declined through time. These are broad relative indicators of successional stage with more biogenic structures present in Stage III communities (Pearson and Rosenberg 1978). Higher successional stages and biogenic structures would be associated with periods of biological processes being dominant. Physical disturbance (primarily from storms) would reset successional stage and controlling the direction of recovery (Trueblood et al. 1994).

Changes in estimated successional stage and biogenic structures may be linked to coarsening of sediments. Both modal grain-size estimated from SPI and median grain-size from grabs significantly coarsened by about one Phi unit in 28 years. For modal Phi, this represents going from an average nearfield grain-size of very-fine-sand-silt (4 to 5 Phi) to fine-sand (4 Phi). For median Phi, the average change was from fine-sand to fine-medium-sand (2 to 3 Phi) (Figure 3-17). Through time the influence of grain-size on successional stage was most prominent within a station (Figure 3-21). Coarsest sediment stations with pebble, gravel, or medium-sand tended to be classified as pioneering Stage I. For example, Stations NF19 and NF23 never had an equilibrium Stage III classification. Stage III fauna occurred primarily at fine-sand and mixed sediment stations. Most years, Stations NF08, NF12, and NF21, which consistently have soft sediments, had Stage III fauna. The largest annual decline in estimated successional stage was associated with the stormiest year of 2013 (as measured by IWaveS Pa h, Codiga et al. 2019) and continued to 2016-2017 when stations returned to pre 2013 successional stages (Figure 3-21). Conversely, the largest increase in successional stage was associated with the seventh stormiest year of 1998. This increase was sustained through subsequent less stormy years (1999, 2000, and 2002) at coarse sediment stations until 2005, the second stormiest year. At most fine grained stations the increased successional stages lasted until 2013, the stormiest year (Figure 3-21).

Much of the change in biological and sediment parameters was related to winter-period storm intensity (sum of IWaveS) and numbers (Figure 3-22). The probability of bed roughness being physically dominated vs. biologically dominated (Figure 3-23) increased significantly as the sum of integrated wave stress (IWaveS) increased (logistic regression, $p = 0.017$). The total number of biogenic structures seen in SPI images tended to decline with the intensity of winter-period storms and also with the number of storms per year (exponential regression, $p = 0.087$). Both of these trends are likely related to storm driven sediment mixing and transport and subsequent changes in sediment grain-size.

Median grain-size across the nearfield coarsened significantly with the increasing number of storms (Figure 3-22). Patterns for individual stations were variable. At Station NF17 (Figure 3-24), a sandy site located about 1 km from the western end of the diffuser, grain-size ranged from fine-sand to medium-coarse-sand with a coarsening of grain-size though time for both modal and median Phi (linear regressions, $p = <0.001$, Figure 3-25). At Station NF12 (Figure 3-26), located 2.4 km to the northwest of the outfall, there was little variation in sediment grain-size through time. It had mixed sediments with a modal grain-size of very-fine-sand to medium-silt (4 to 6 Phi). Median grain-size was slightly coarser and ranged from very-fine-sand to coarse-silt (4 to 5 Phi). Station NF12 was consistently the finest grained of the 23 nearfield stations.

Community Patterns

Patterns in infaunal abundance and species were also related to time (year) and winter-period storm intensity (sum of IWaveS from October to May). The two stations sampled in every year of the 28-year monitoring period were examined to assess infaunal patterns. Station NF17 (Figure 3-24) was sandy and Station NF12 (Figure 3-26) contained mixed sediments.

Station NF17

Total infaunal abundance at Station NF17 was variable, which is typical of infauna. Highest peaks in abundance occurred prior to outfall operation with no significant trend though time (Figure 3-27). Abundance was related to the intensity of winter-period storms with fewer individuals occurring in stormy years (exponential regression, p = <0.001) (Figure 3-27). The six most abundant species over the 28-years of monitoring made up 52% of the total, spanned a ten-fold range in maximum abundance, and each exhibited a different temporal pattern (Figure 3-28).

The most abundant species at NF17 was the amphipod *Crassicorophium crassicorne*, a tube-builder that prefers sandy sediments (Hilbig and Blake 2000). It peaked three times over the 28-year monitoring period, twice prior to outfall operation and again between the high storm years of 2005 and 2010 (Figure 3-28). The abundance of *Crassicorophium crassicorne* was related to the intensity of winter-period storms with the lowest abundance occurring on the highest storm years (exponential regression, p = 0.020) (Figure 3-29). On high abundance years, *Crassicorophium crassicorne* tubes dominated the sediment surface. It formed tube mats on the sediment surface in 2003, 2008, and 2019 (Figure 3-30). Variation in the annual abundance of *Polygordius jouinae, Spiophanes bombyx*, and *Exogone hebes*, the second, third, and fourth most abundant species, was not related to time or storm intensity (Figures 3-28 and 3-29).

The fifth most abundant species was *Pseudunciola obliquua*, a burrowing amphipod that prefers sandy sediments and is one of the most abundant amphipods on shallow continental shelfs (Morgan and Woodhead 1984). It was abundant at NF17 prior to outfall operation and declined to near zero until 2019 (Figure 3-28). Its abundance was related to the intensity of winter-period storms with lowest numbers occurring on highest storm years (polynomial regression, p = 0.050) (Figure 3-29). The sixth most abundant species was *Parvicardium pinnulatum*, a small cockle that prefers muddy sandy sediments mixed with gravel (Ballerstedt 2005). Its peak abundance was prior to outfall operation with variable abundance up to 2013 following which it was consistently low through to 2019 (Figure 3-28). Its abundance was related to the intensity of winter-period storms with lowest numbers occurring on highest storm years (polynomial regression, p = 0.034) (Figure 3-29).

Station NF12

At Station NF12 total infaunal abundance was variable and tended to be higher prior to outfall operation up to 2004 (Figure 3-31). In 2005, the second stormiest year, abundance declined and remained lower through 2019. Total abundance at NF12 was marginally related to the intensity of winter-period storms and tended to be lower on higher storm years (logarithmic regression, p = 0.102) (Figure 3-31). The six most abundant species over the 28-years of monitoring were 79% of the total, spanned a five-fold range in maximum abundance, and each exhibited a different temporal pattern (Figure 3-32).

The most abundant species at NF12 was the polychaete *Mediomastus californiensis*, a burrowing subsurface deposit feeder (Hilbig and Blake 2000), overall making up about 16% of the total abundance. It was consistently present over the 28 years with a long-term average of 352 individuals/0.04 m^2 and a coefficient of variation (CV) of 35%, but had a declining trend from 1992 to 2012 (polynomial regression, p = 0.007). From 2013 on, its numbers increased (Figure 3-32). Patterns in *Mediomastus californiensis* abundance were not related to winter-period storm intensity (Figure 3-33).

Prionospio steenstrupi, the second most abundant species at NF12, is an interface feeding, tube-building polychaete. It had one peak in abundance from about 2002 to 2004 (Figure 3-32). From 2005 on it declined with a slight rise again in 2019. The abundance of *Prionospio steenstrupi* tended to be lower with higher winter-period storm intensity (power regression, p = 0.064) (Figure 3-33). The number of tubes observed in SPI tended to be higher when *Prionospio steenstrupi* was abundant (Figure 3-34).

The third most abundant species was *Spio limicola*, an interface feeding polychaete, which declined from its highest abundance in the 1990s through to 2019 (exponential regression of abundance with year, p = <0.001). The high degree of variability (CV = 119%) in its abundance obscured a possible relationship with intensity of winter-period storms. *Spio limicola* abundance in 1994 spiked by more than a factor of 4. With 1994 removed it tended to decline with increasing storm intensity (logarithmic regression of abundance with IWaveS sum, 1994 excluded, p = 0.060).

Tharyx acutus, a small, free-burrowing, surface deposit feeding polychaete, was the fourth most abundant species. It had two peaks in abundance over the monitoring years centered around 2001 to 2003 and 2012 to 2014. The decline of the first peak was coincident with the second highest storm year of 2005. The second peak increased through 2013 (first stormiest year) and declined in 2015 (sixth stormiest year) (Figure 3-32). The abundance of *Tharyx acutus* tended to be highest during low intensity winter-period storm years, with the exception of 2013 (Figure 3-33). Had it not increased in 2013 it would have declined with increasing storm intensity (logarithmic regression, 2013 excluded, p = 0.032).

The fifth most abundant species was *Levinsenia gracilis*, burrowing subsurface feeding polychaete. It was the only top dominant species to increase in abundance through the monitoring period (exponential regression, p = <0.001). Its abundance was not related to winter-period storm intensity (Figures 3-32 and 3-33).

Aricidea catherinae, a burrowing subsurface feeding polychaete, was the sixth most abundant species. Its abundance declined from 1993 to 2000 and then peaked from 2001 to 2003 (Figure 3-32). From 2005 (second stormiest year) to 2015 (sixth stormiest year) its abundance was consistency low and then its abundance increased through 2018 (fourth stormiest year). Overall, its abundance did decline and increase again (polynomial regression, p = <0.001), but was not related to winter-period storm intensity (Figure 3-33).

In aggregate, this evaluation of infaunal species abundances tends to support the strong linkages observed between storminess and sediment profile imaging parameters.

Table 3-5. Summary of SPI parameters pre- and post-baseline years for all nearfield stations.

	Baseline Years 1992-2000 9-Year Interval	**Outfall Operational Years 2001-2019 19-Year Interval**	**Only 2019**
SS	Advanced from I to II-III	Bimodal: II-III tending to I	Bimodal: I-II and I
OSI - Low	4.8 (1997)	5.8 (2003)	
OSI - High	7.2 (2000)	8.7 (2012)	8.3 (N = 22)
RPD - Low	1.8 cm (1997 and 1998)	2.1 cm (2003)	
RPD -High	3.0 cm (1995)	5.5 cm (2015)	
Annual Mean RPD Measured	2.2 (0.48 SD) cm	3.8 (1.06 SD) cm	4.8 (0.8 SD) cm N = 15
Annual Mean RPD All Values	2.4 (0.47 SD) cm	3.4 (0.98 SD) cm	4.9 (1.4 SD) cm N = 23

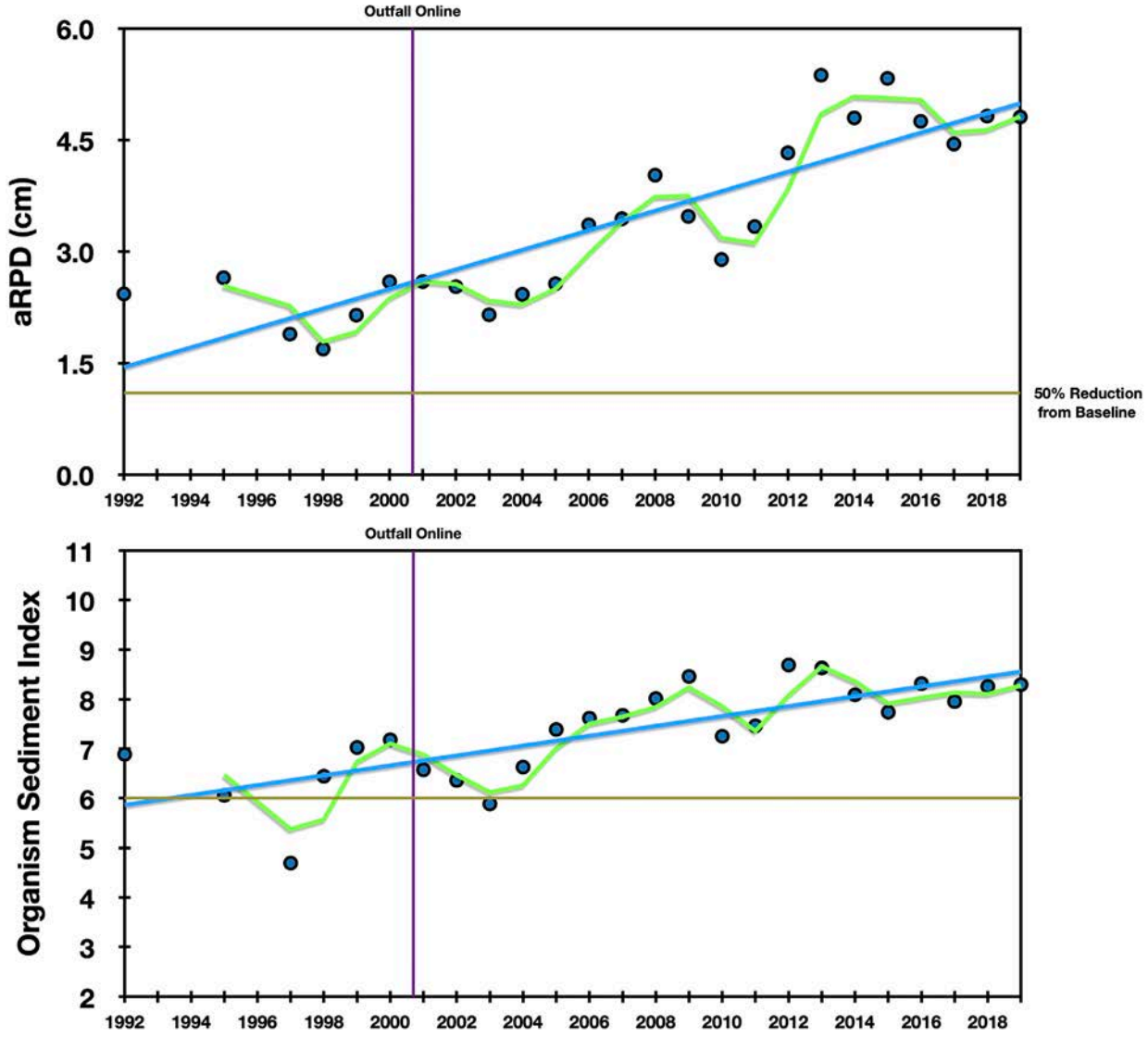

Figure 3-16. Trends in apparent color redox-potential discontinuity (aRPD) layer depth and organism sediment index (OSI) through time. Points are average for all 23 nearfield stations. Green line is two-year moving average. Blue line is linear regression line. OSI <6 indicates poor habitat quality.

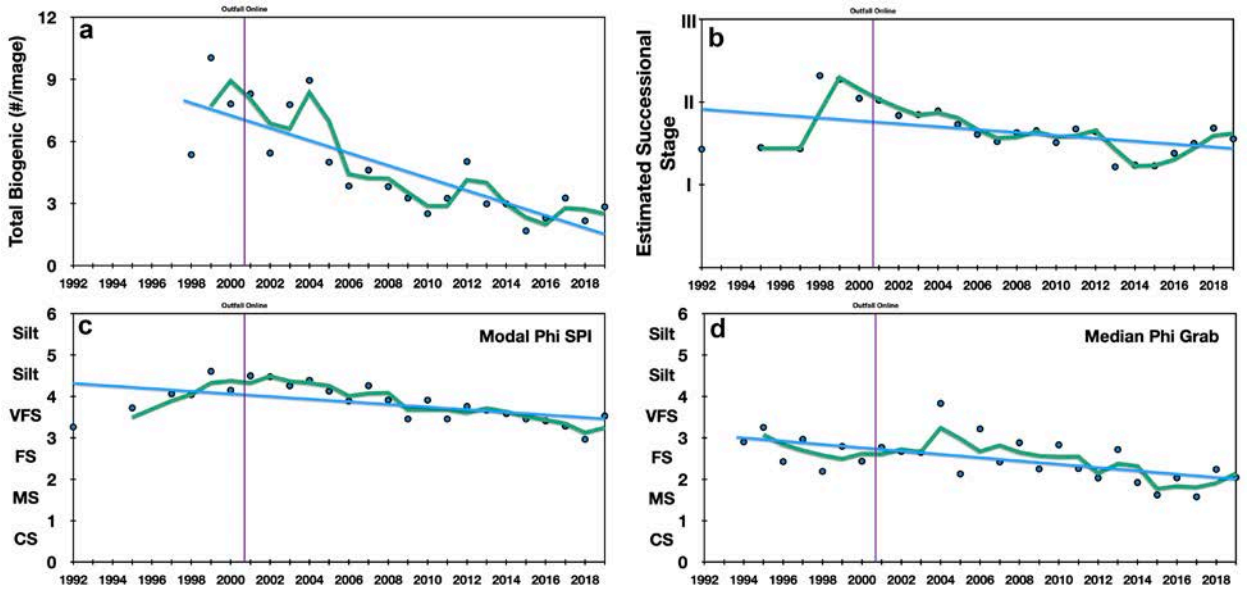

Figure 3-17. Trends in SPI parameters and grain-size through time. a) total biogenic structures is the sum of infauna, burrows, and voids per image, b) estimated successional stage I is pioneering, III is equilibrium, and II is intermediate, c) modal grain-size estimated from images, d) median grain-size estimated from grab samples. CS is coarse-sand, FS is fine-sand, MS is medium-sand, VFS is very-fine-sand. Points are average for all 23 nearfield stations. Green line is two-year moving average. Blue line is linear regression line.

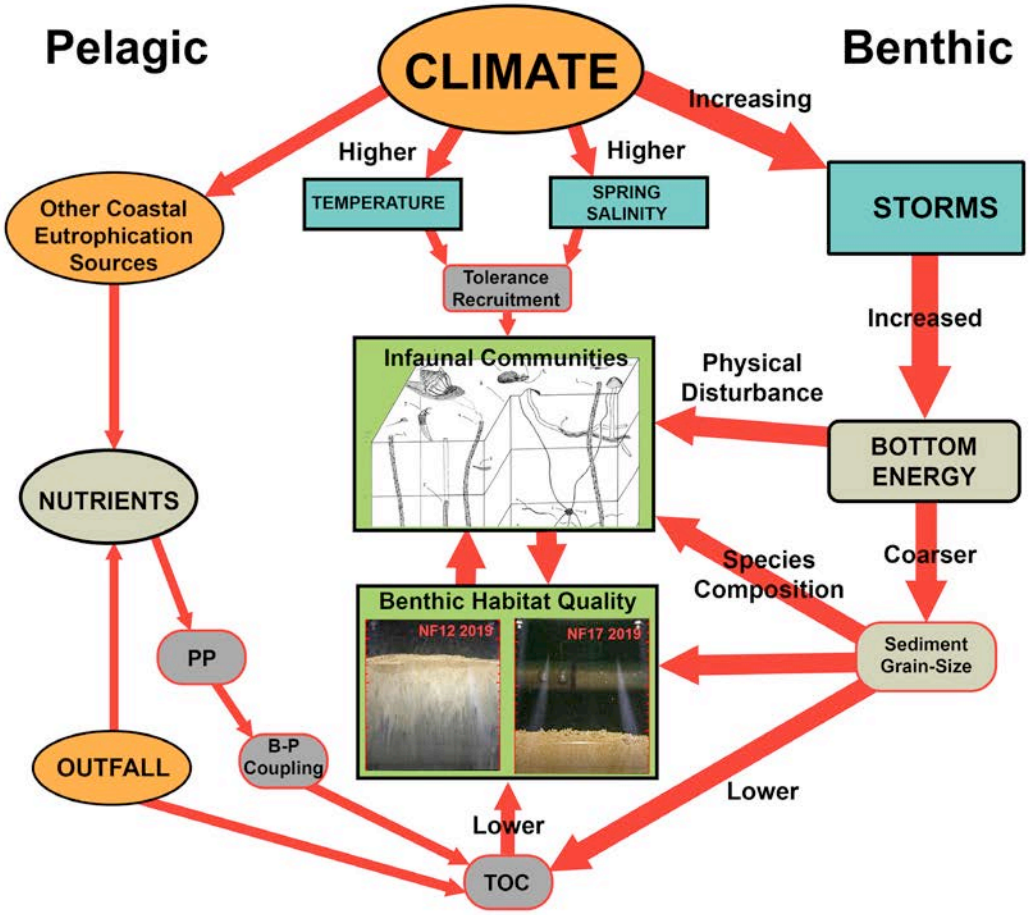

Figure 3-18. Conceptual model of major driving factors effecting benthic and pelagic ecosystems in the nearfield monitoring area.

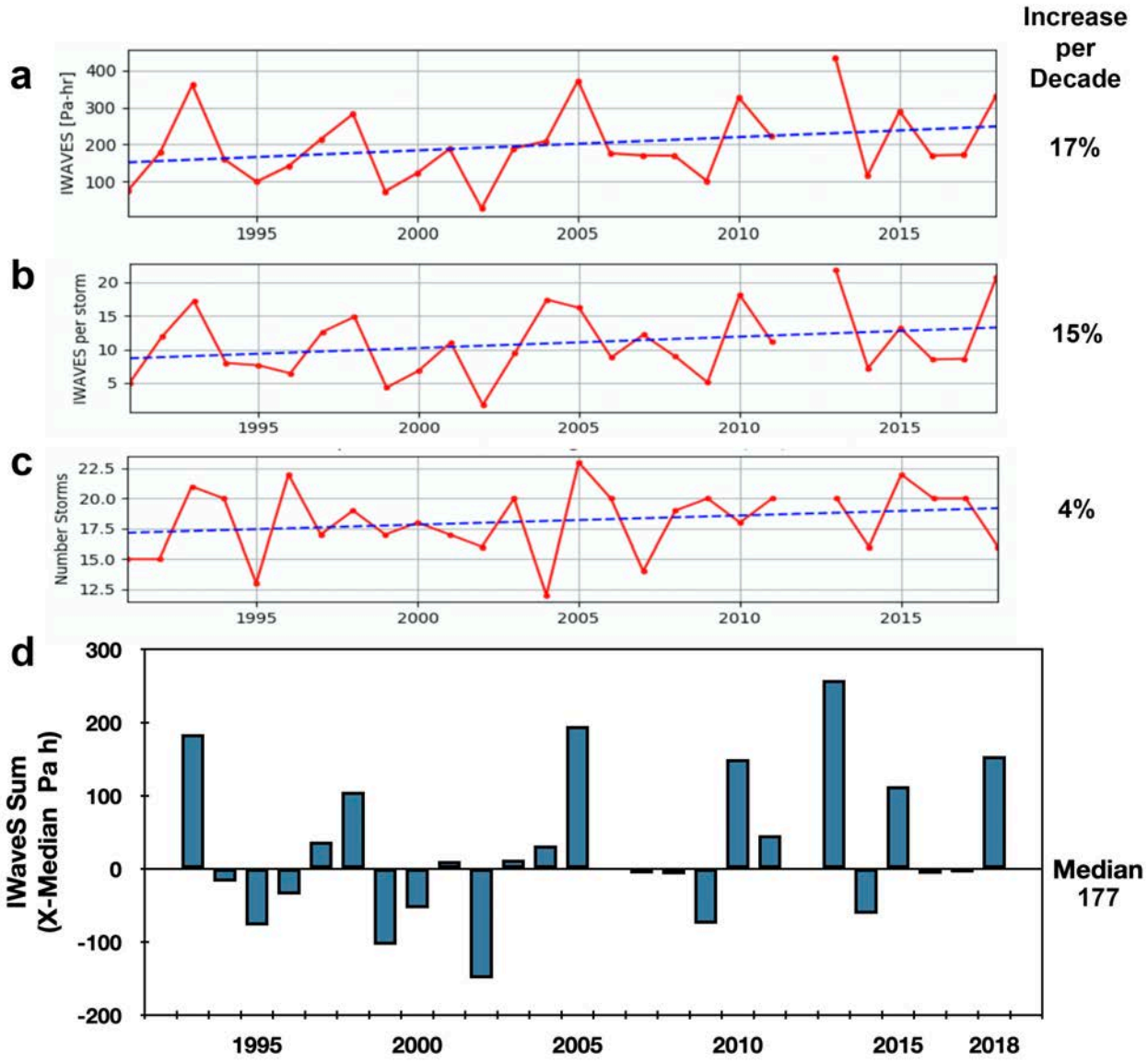

Figure 3-19. Long-term climate driven changes in winter-period (October to May) storm intensity and number from 1990 to 2018 (Codiga et al. 2019). a) sum of integrated wave stress (IWaveS), b) average IWaveS per storm, c) number of storms, d) annual IWaveS anomaly based on median. Increase per decade based on linear regression (dashed lines).

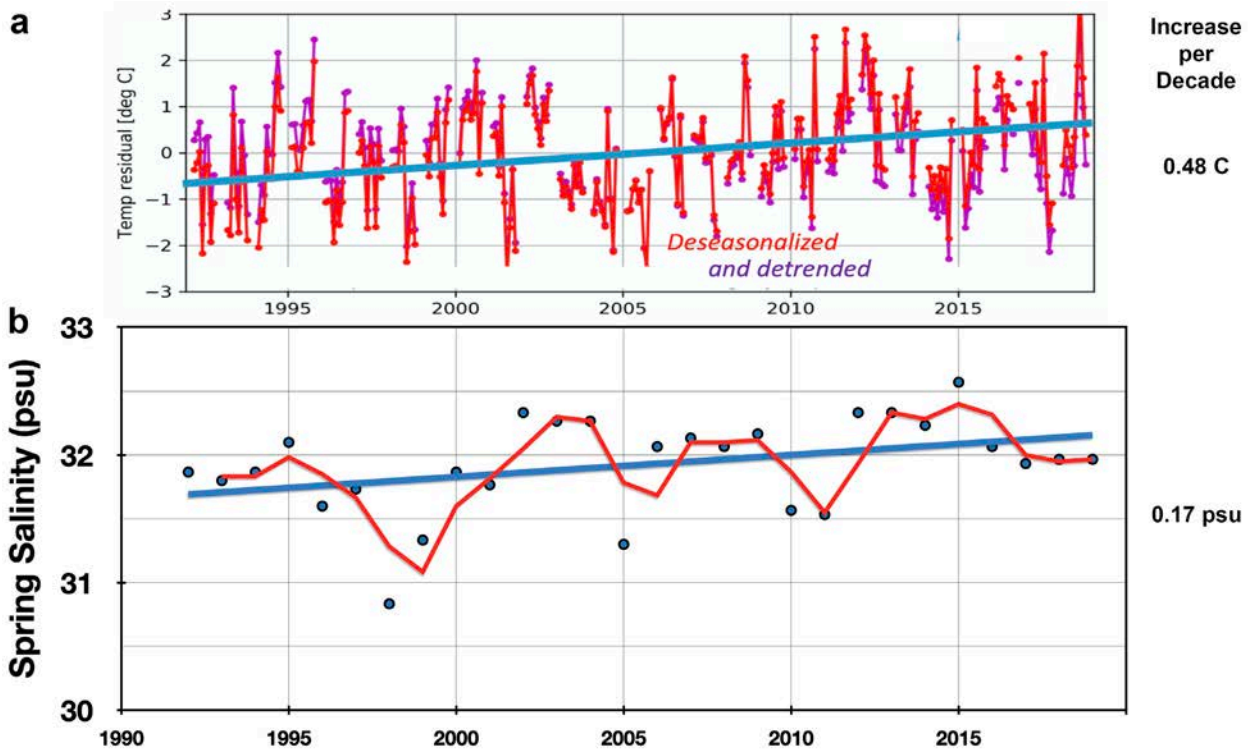

Figure 3-20. Long-term climate driven changes in temperature and salinity (MWRA monitoring database, Codiga et al. 2019). a) temperature for months of February to October, b) salinity for spring months March to May. Increase per decade based on linear regression (blue lines).

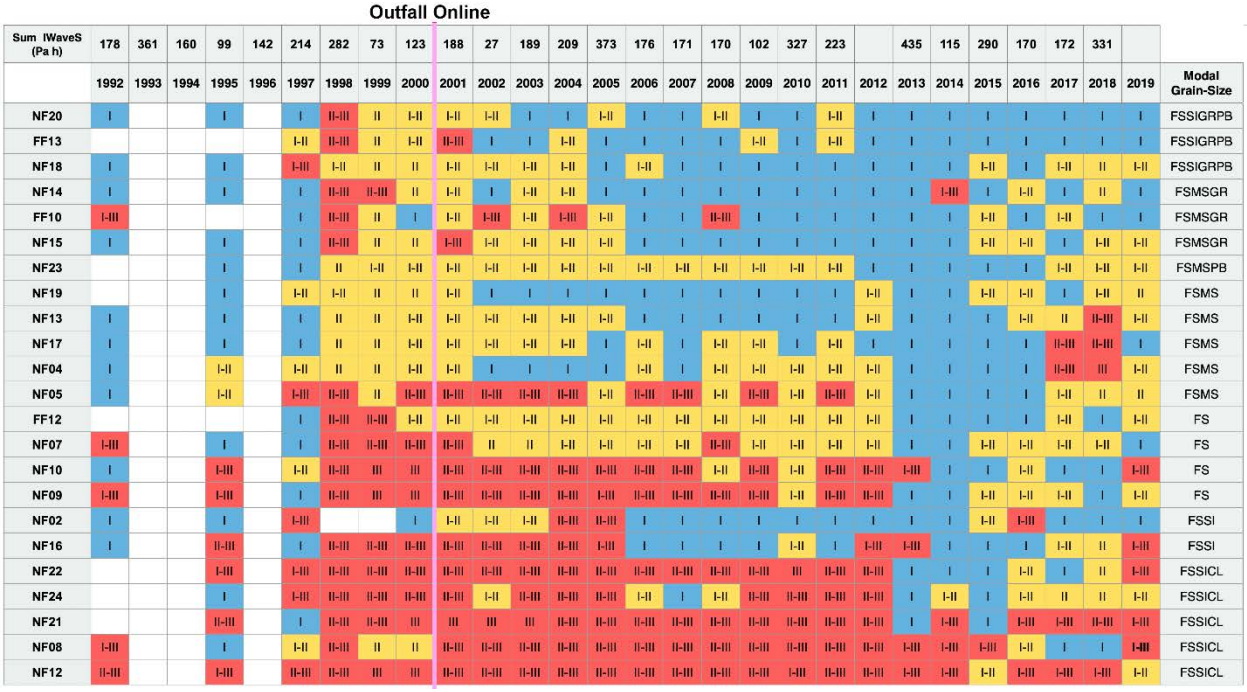

Sum IWaveS (Pa h)	178	361	160	99	142	214	282	73	123	188	27	189	209	373	176	171	170	102	327	223		435	115	290	170	172	331		
	1992	1993	1994	1995	1996	1997	1998	1999	2000	2001	2002	2003	2004	2005	2006	2007	2008	2009	2010	2011	2012	2013	2014	2015	2016	2017	2018	2019	Modal Grain-Size
NF20	I			I		I	II-III	II	I-II	I-II	I-II	I	I	I-II	I	I	I-II	I	I	I-II	I	I	I	I	I	I	I	I	FSSIGRPB
FF13						I-II	II-III	II	I-II	II-III	I	I	I-II	I	I	I	I	I-II	I	I-II	I	I	I	I	I	I	I	I	FSSIGRPB
NF18	I			I		I-III	I-II	II	II	I-II	I-II	I-II	I-II	I	I-II	I	I	I	I	I	I	I	I	I-II	I	I-II	II	I-II	FSSIGRPB
NF14	I			I		I	II-III	II-III	II	I-II	I	I-II	I-II	I	I	I	I	I	I	I	I	I	I-III	I	I-II	I	II	I	FSMSGR
FF10	I-III					I	II-III	II	I	I-II	I-III	I-II	I-III	I-II	I	I	II-III	I	I	I	I	I	I	I-II	I	I-II	I	I	FSMSGR
NF15	I			I		I	II-III	II	II	I-III	I-II	I-II	I-II	I-II	I	I	I	I	I	I	I	I	I	I-II	I-II	I	I-II	I-II	FSMSGR
NF23				I		I	II	I-II	I-II	I-II	I-II	I-II	I-II	I-II	I-II	I-II	I-II	I-II	I-II	I-II	I	I	I	I	I	I-II	I-II	I-II	FSMSPB
NF19				I		I-II	I-II	II	II	I-II	I	I	I	I	I	I	I	I	I	I	I-II	I	I	I-II	I-II	I	I-II	II	FSMS
NF13	I			I		I	II	II	I-II	I-II	I-II	I-II	I-II	I-II	I	I	I	I	I	I	I-II	I	I	I	I-II	II	II-III	I-II	FSMS
NF17	I			I		I	II	II	I-II	I-II	I-II	I-II	I-II	I	I-II	I	I-II	I-II	I	I-II	I	I	I	I	I	II-III	II-III	I	FSMS
NF04	I			I-II		I-II	II	II	I-II	I-II	I	I	I	I	I-II	I	I-II	I-II	I-II	I-II	I-II	I	I	I	I	II-III	III	I-II	FSMS
NF05	I			I-II		I-III	II-III	II	II-III	II-III	II-III	II-III	II-III	I-II	II-III	II-III	I-II	II-III	I-II	II-III	I-II	I	I	I	I	I-II	II	II	FSMS
FF12						I	II-III	II-III	I-II	I-II	I-II	I-II	I-II	I-II	I-II	I-II	I-II	I-II	I-II	I-II	I-II	I	I	I	I	I-II	I	I-II	FS
NF07	I-III			I		I	II-III	II-III	II-III	II-III	II	II	I-II	I-II	I-II	I-II	II-III	I-II	I-II	I-II	I-II	I	I	I-II	I-II	I-II	I-II	I	FS
NF10	I			I-III		I-II	II-III	III	III	II-III	II-III	II-III	II-III	II-III	II-III	II-III	I-II	II-III	I-II	II-III	II-III	I-III	I	I	I-II	I	I	I-III	FS
NF09	I-III			I-III		I	II-III	III	III	II-III	II-III	II-III	II-III	I-III	II-III	II-III	II-III	II-III	I-II	II-III	II-III	I	I	I-II	I-II	I-II	I	I-II	FS
NF02	I			I		I-III			I	I-II	I-II	I-II	II-III	II-III	I	I	I	I	I	I	I	I	I	I-II	I-III	I	I	I	FSSI
NF16	I			II-III		I	II-III	II-III	II-III	II-III	II-III	II-III	II-III	I-III	I	I	I	I	I-II	I	I-III	I-III	I	I	I	I-II	II	I-III	FSSI
NF22				I-III		I-III	II-III	II-III	II-III	II-III	II-III	II-III	II-III	II-III	II-III	II-III	II-III	II-III	III	II-III	II-III	I	I	I	I-II	I	II	I-III	FSSICL
NF24				I		I-III	II-III	II-III	II-III	II-III	I-II	II-III	II-III	II-III	I-II	I	I-II	II-III	II-III	II-III	II-III	I	I-II	I	I-II	II	II	I-II	FSSICL
NF21				II-III		I	II-III	II-III	III	III	III	III	II-III	II-III	II-III	II-III	II-III	II-III	II-III	II-III	II-III	I	I-III	I	I-III	I-III	II-III	I-III	FSSICL
NF08	I-III			I		I-II	II-III	II	II	II-III	II-III	II-III	II-III	II-III	II-III	II-III	II-III	II-III	II-III	II-III	II-III	I-III	I-III	I-III	I-II	I	I	I-III	FSSICL
NF12	II-III			I-III		II-III	II-III	III	III	II-III	II-III	II-III	II-III	II-III	II-III	II-III	II-III	II-III	I-III	II-III	II-III	I-III	I-III	I-II	I-III	I-III	I-III	I-II	FSSICL

Figure 3-21. Matrix of estimated successional stage through time. Stations are arranged from coarsest to finest sediments. I is pioneering stage, III is equilibrium stage, and II is intermediate. CL is clay, FS is fine-sand, GR is gravel, MS is medium-sand, PB is pebble, SI is silt.

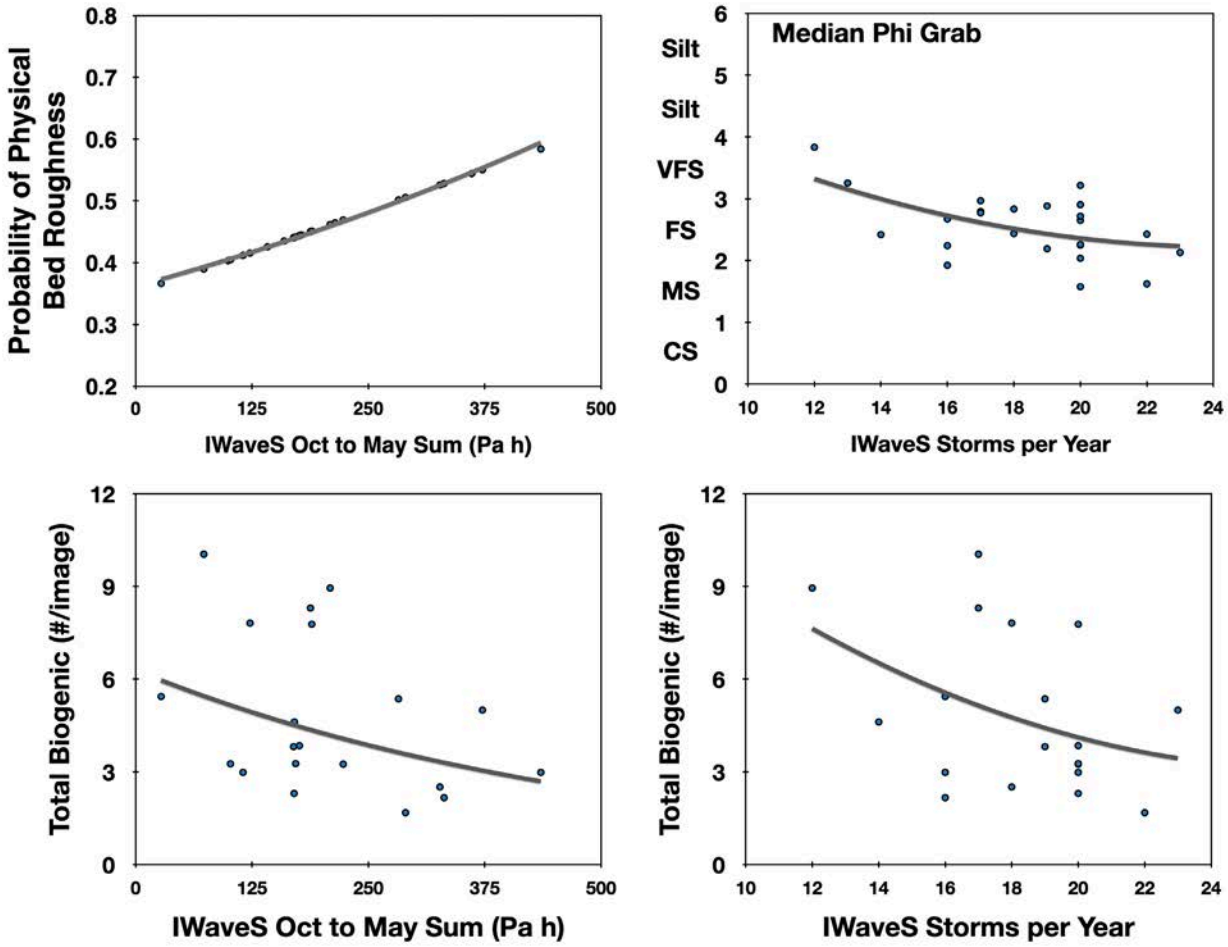

Figure 3-22. Relationships between winter-period storms, and SPI and sediment parameters. CS is coarse-sand, FS is fine-sand, MS is medium-sand, VFS is very-fine-sand. Points are average for all 23 nearfield stations for all years.

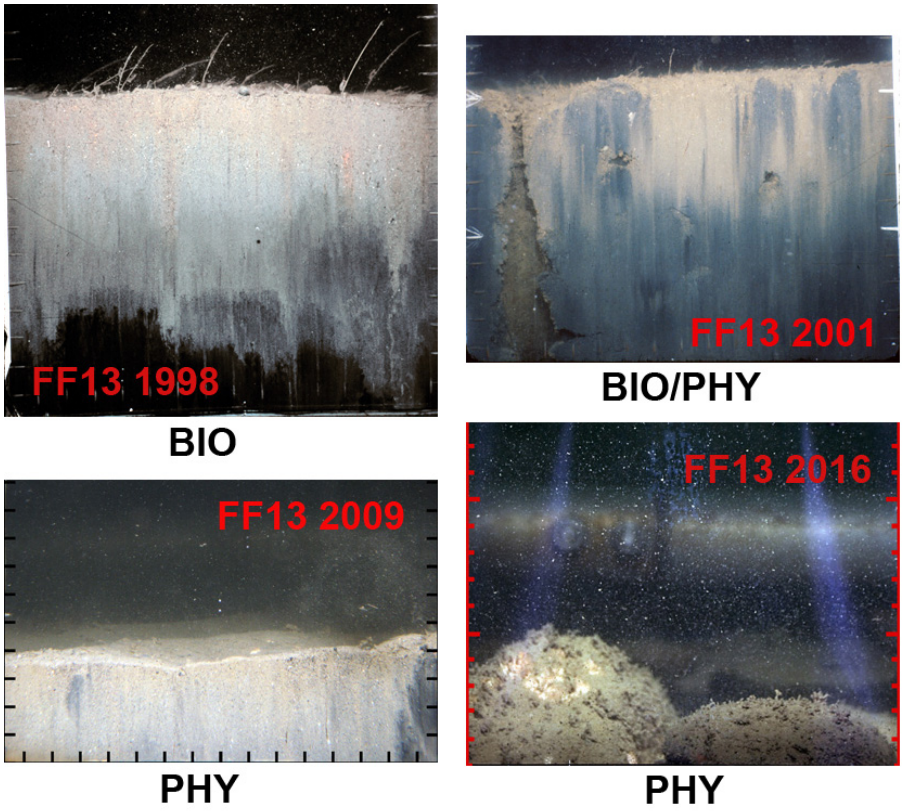

Figure 3-23. Shift in dominance of processes structuring surface sediments at station FF13 through time. BIO is biological dominance, BIO/PHY is combination of biological and physical dominance, PHY is physical dominance. Scale on side of images is in cm.

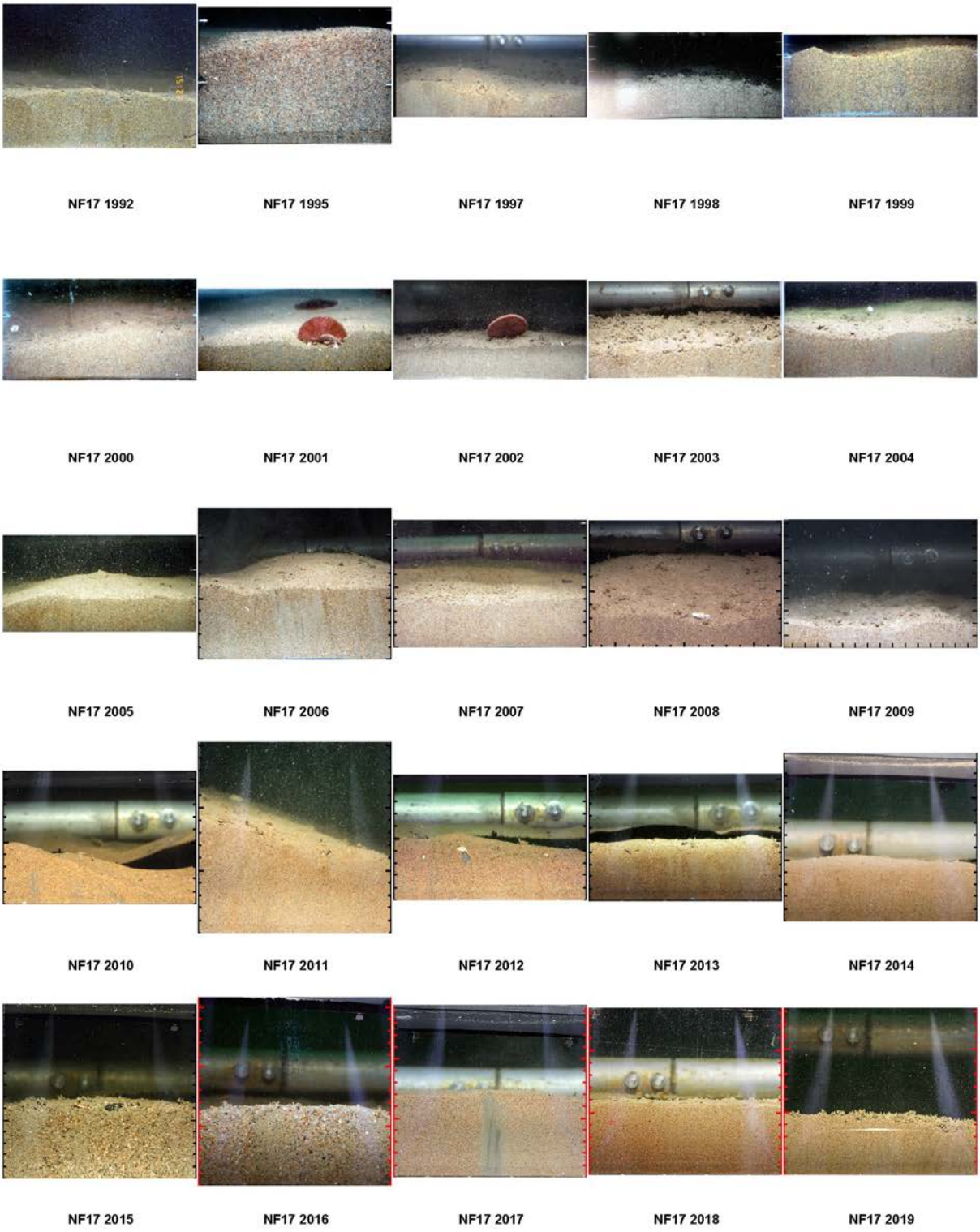

Figure 3-24. Mosaic of SPI images for Station NF17 where sediments coarsened thought time. Scale on side of images is in cm.

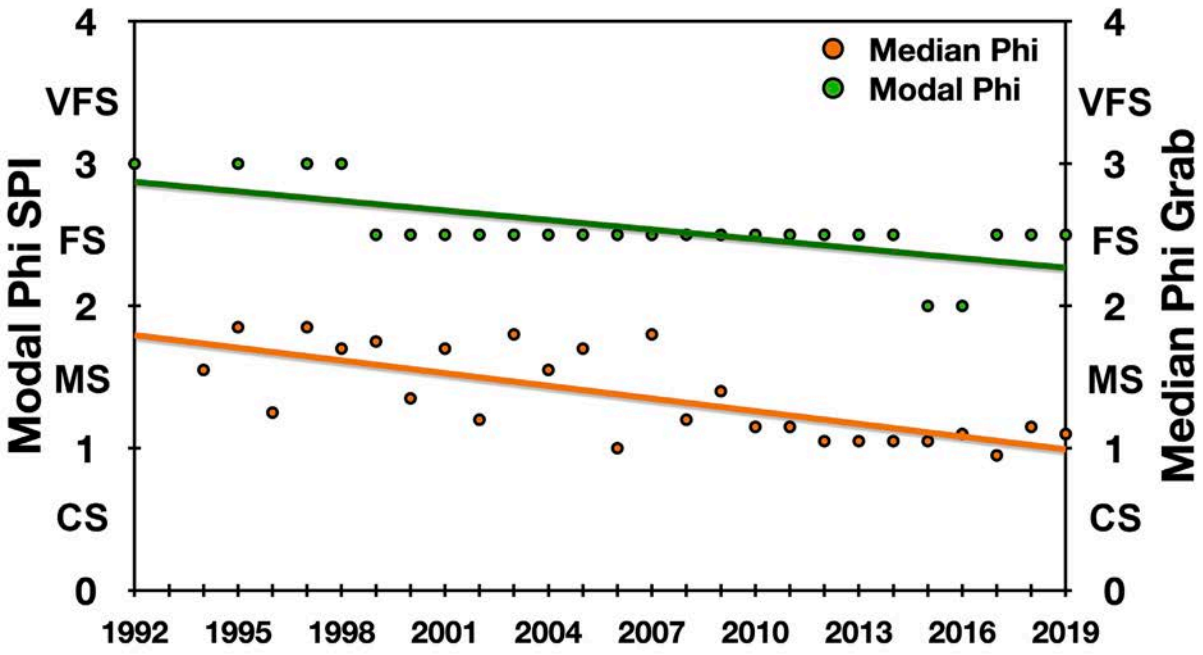

Figure 3-25. Coarsening of modal from SPI images and median sediment grain-size from grab samples at Station NF17.

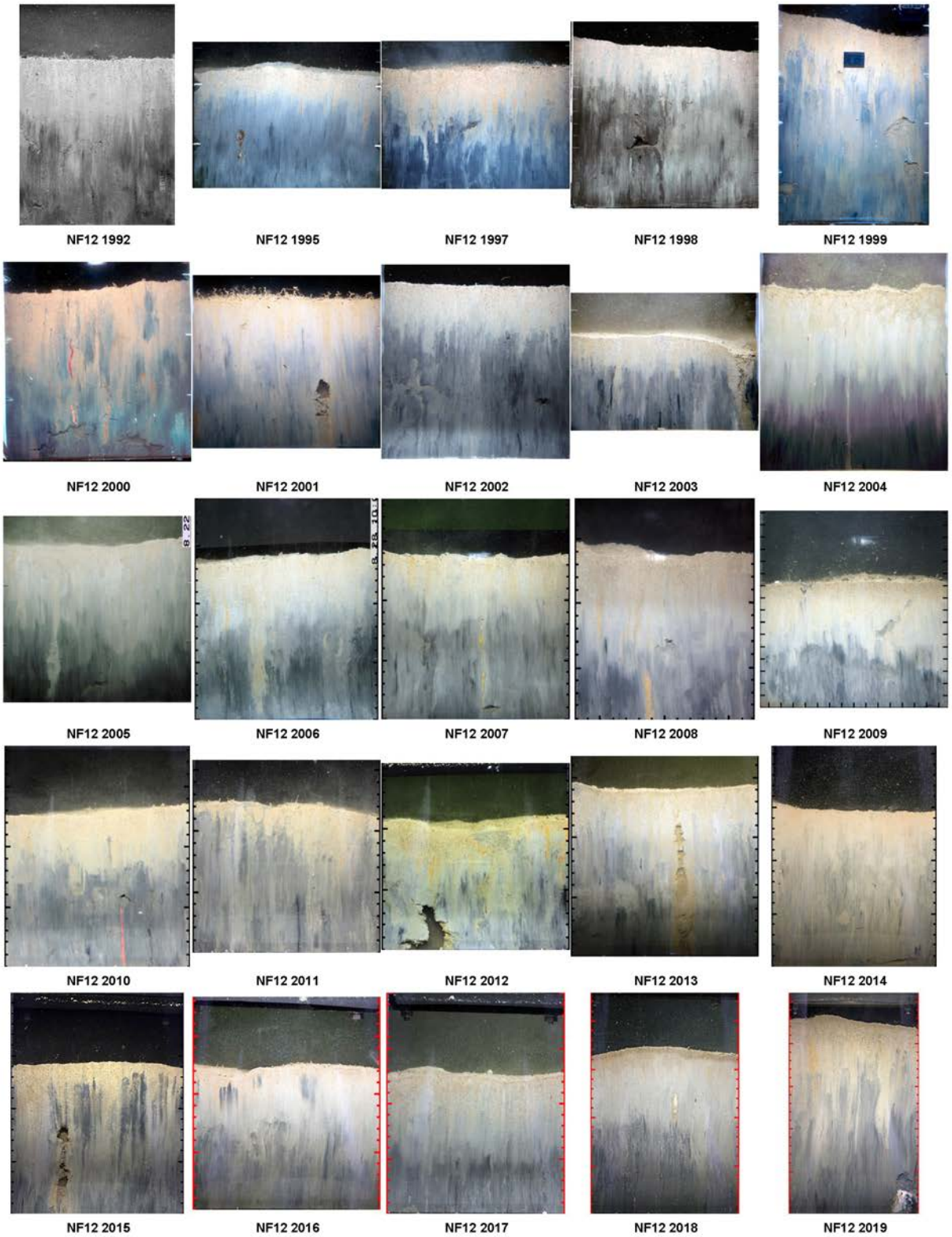

Figure 3-26. Mosaic of SPI images for Station NF12 with mixed fine-sand-silt-clay sediments. Scale on side of images is in cm.

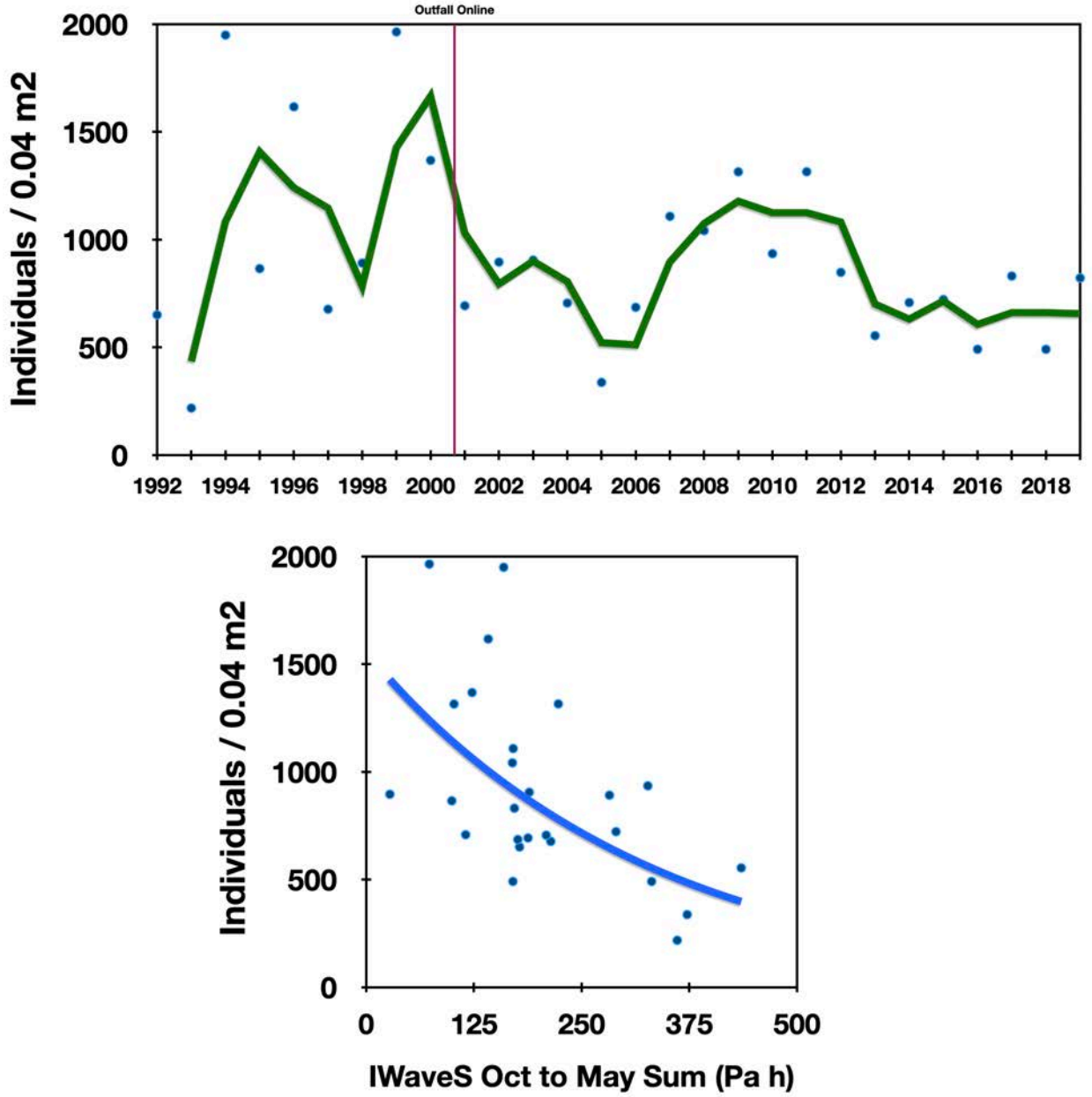

Figure 3-27 Total infaunal abundance at Station NF17 and relationships with storm intensity. Green line is two-year moving average. Blue line is exponential regression line.

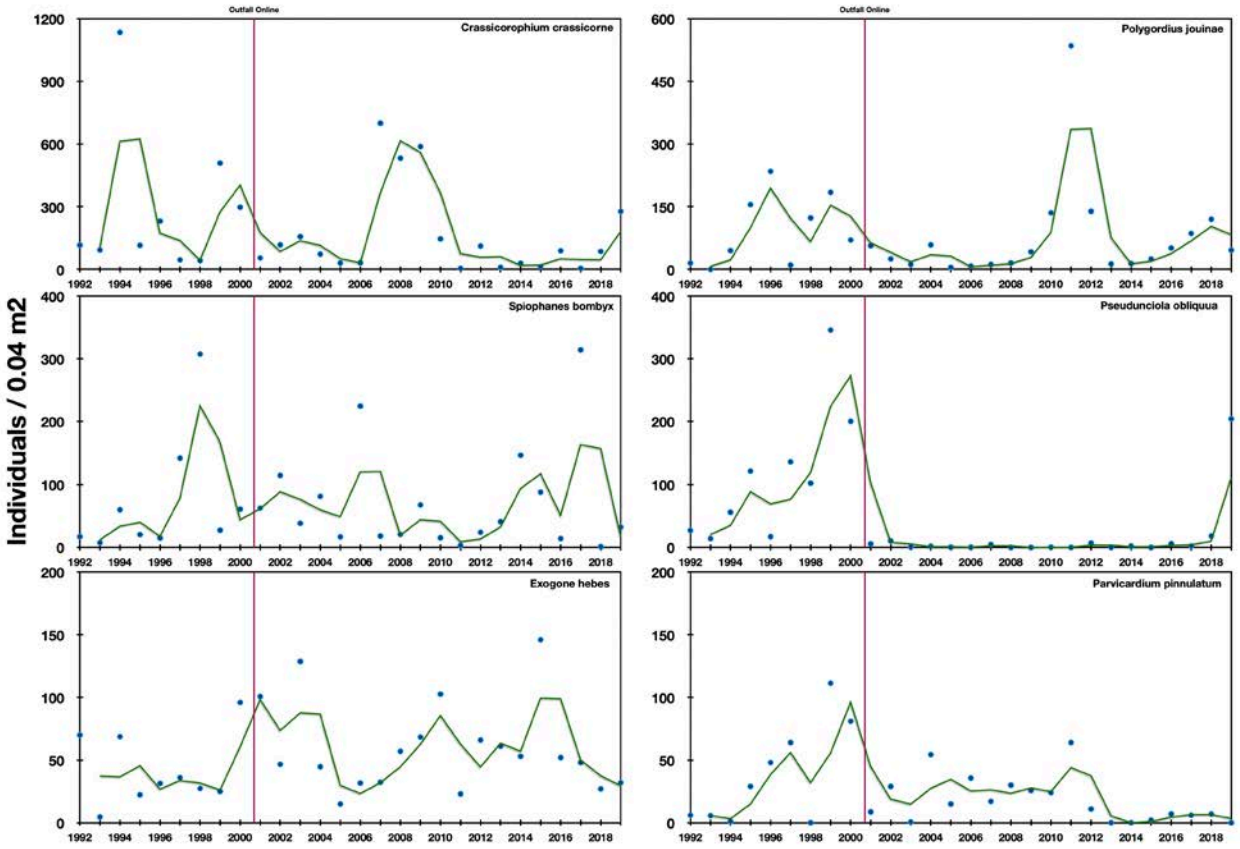

Figure 3-28 Abundance patterns for top six species at sandy Station NF17. Green lines are two-year moving average.

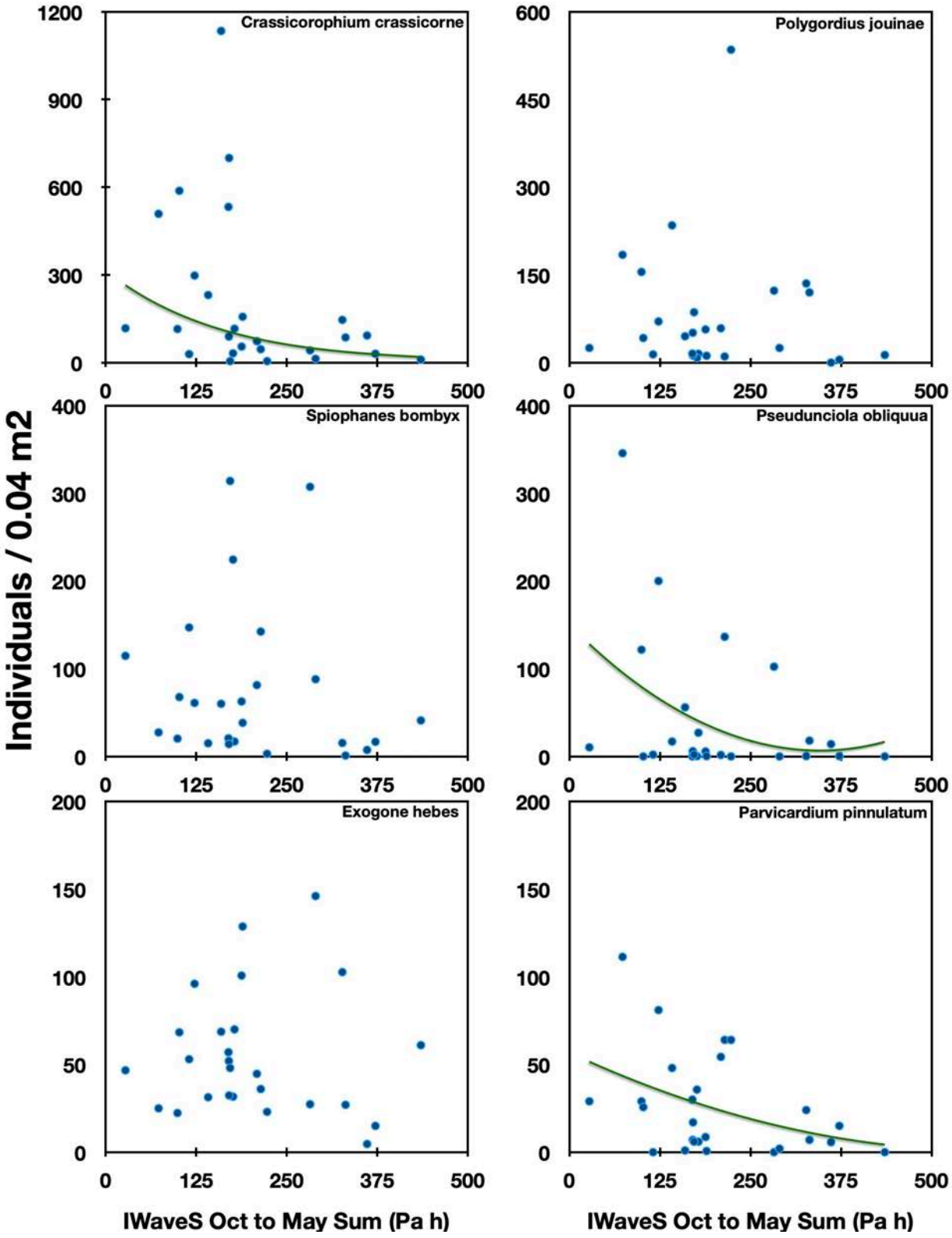

Figure 3-29 Relationships between abundance and winter-period storm intensity for top six species at sandy Station NF17. Regression lines are drawn for significant relationships.

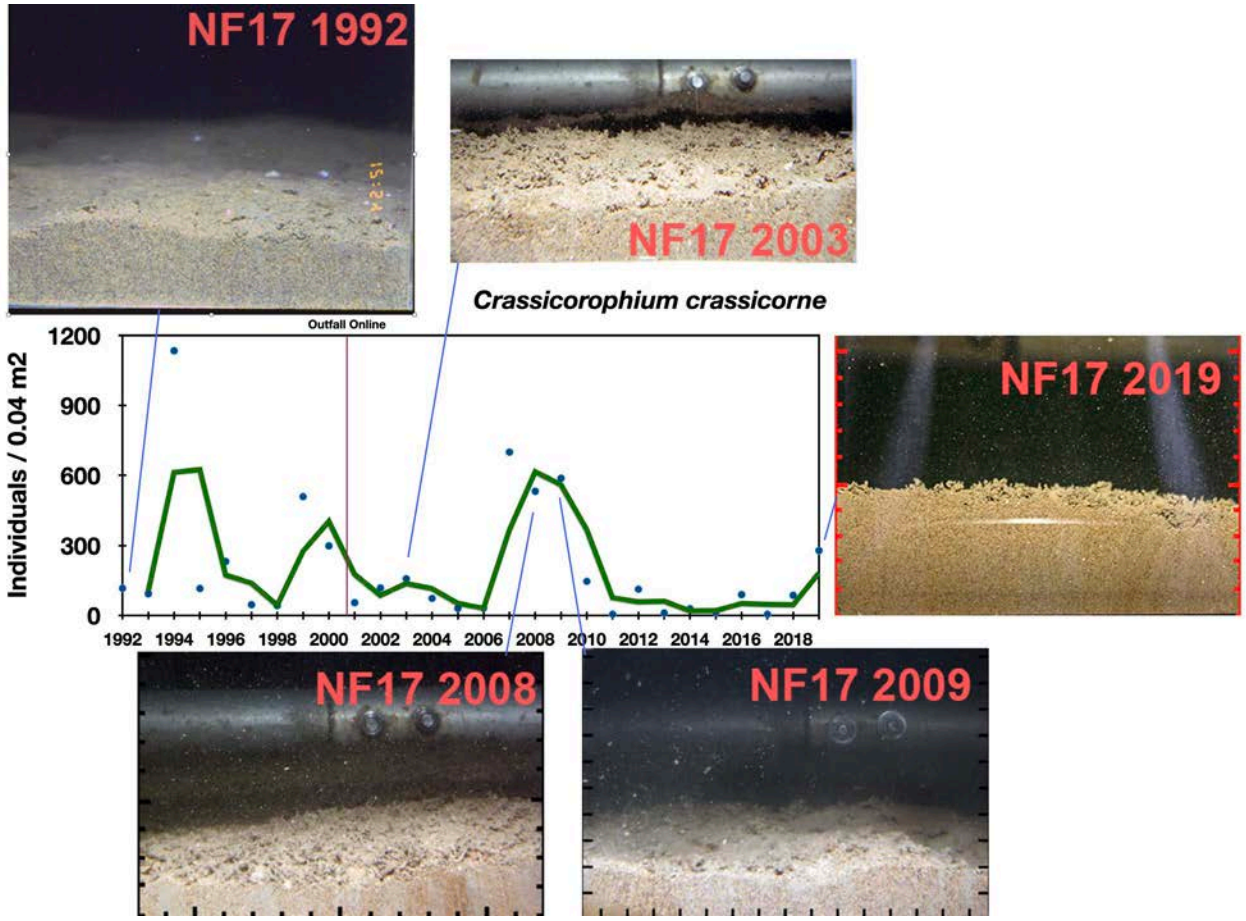

Figure 3-30 Tubes of the amphipod Crassicorophium crassicorne at sandy Station NF17. Green line is two-year moving average.

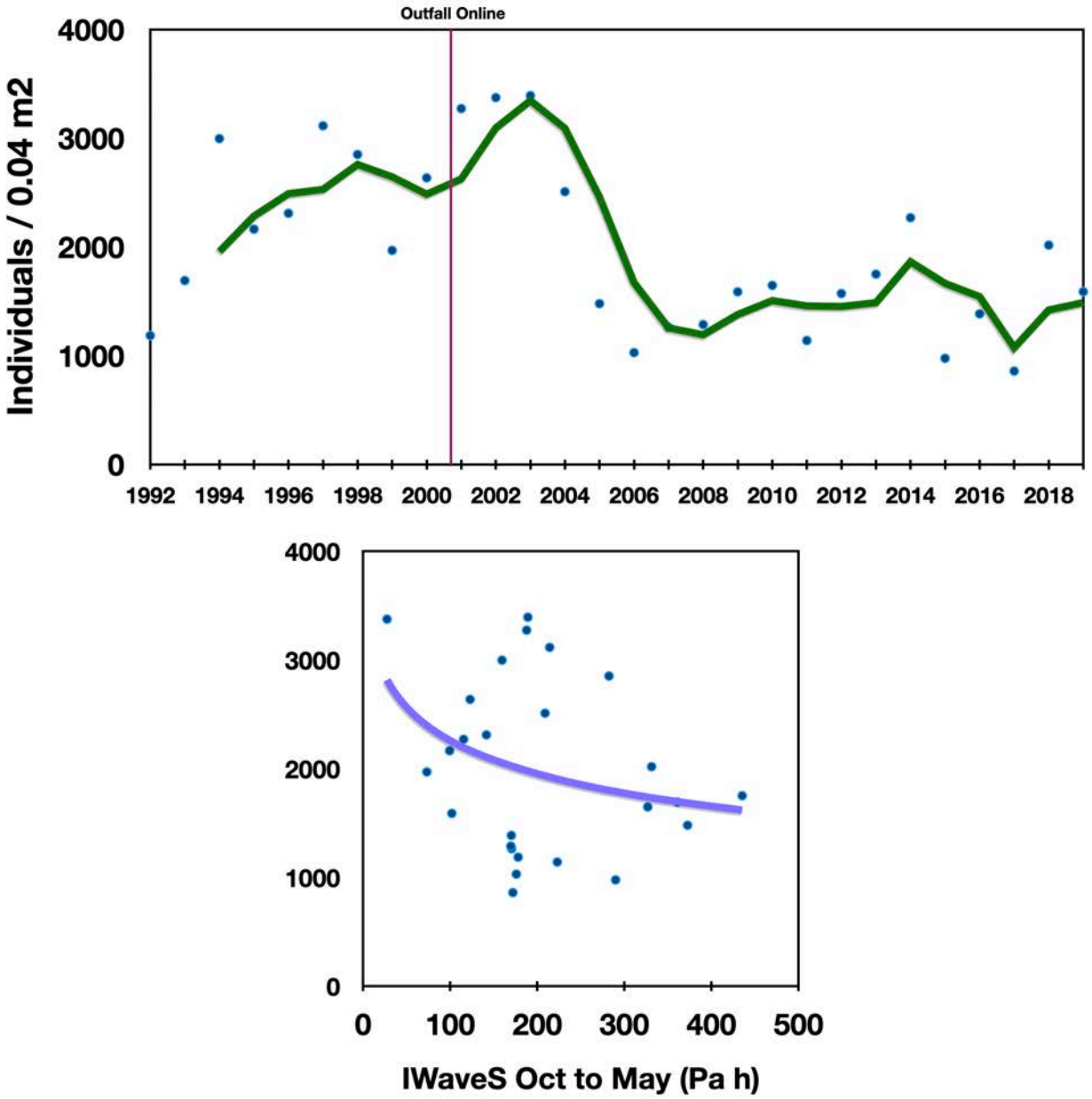

Figure 3-31 Total infaunal abundance at Station NF12 and relationships with storm intensity. Green line is two-year moving average. Purple line is logarithmic regression line.

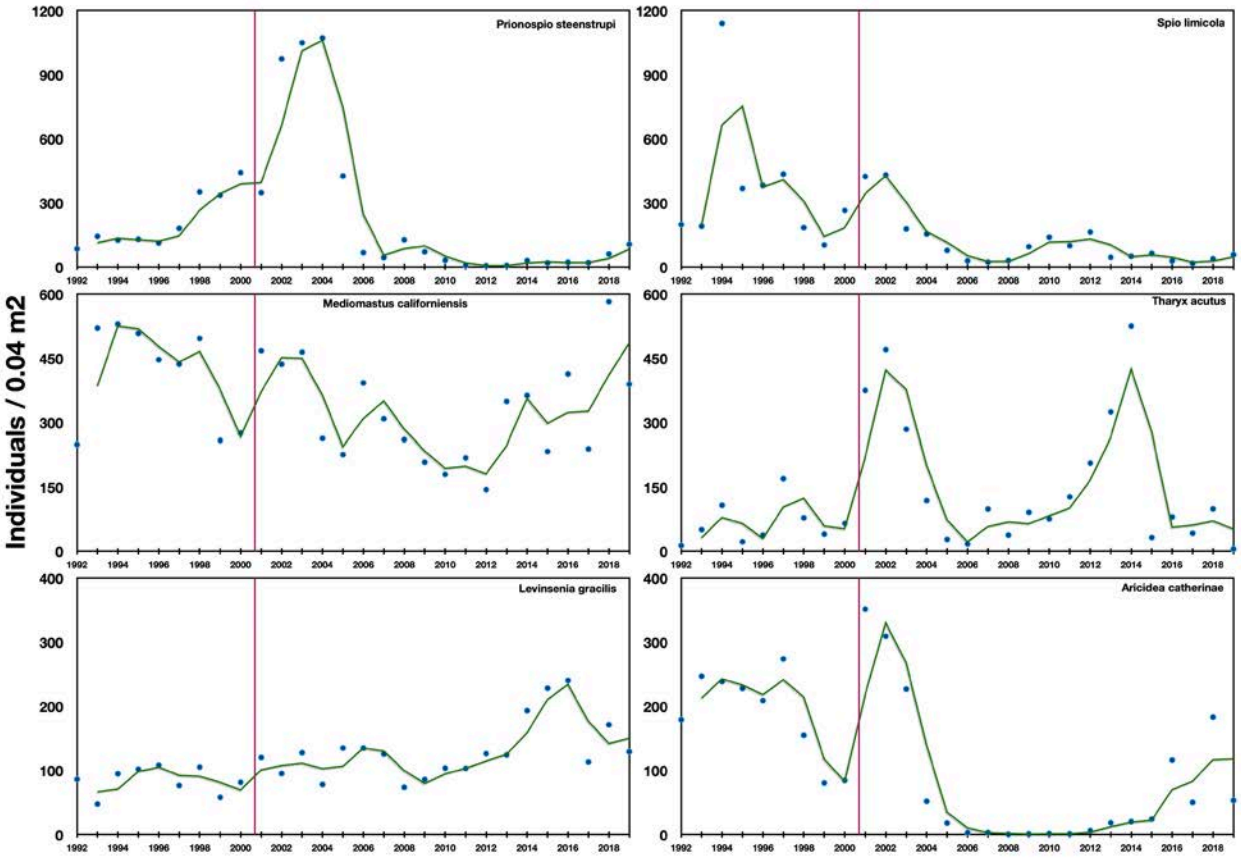

Figure 3-32 Abundance patterns for top six species at mixed sediment Station NF12. Green line is two-year moving average.

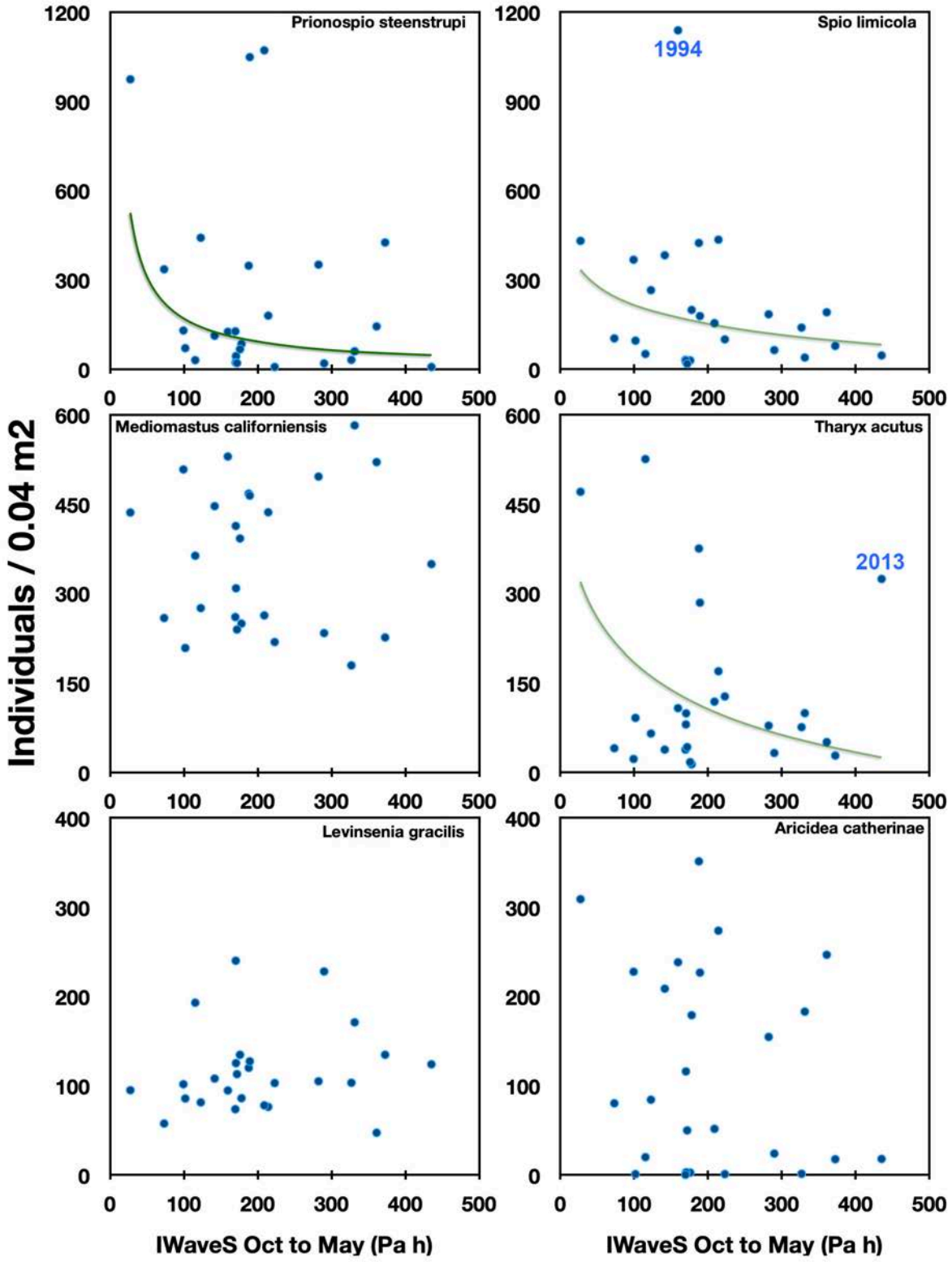

Figure 3-33 Relationships between abundance and winter-period storm intensity for top six species at mixed sediment Station NF12. Regression lines are drawn for significant relationships. Labeled years were considered outliers and excluded from regressions.

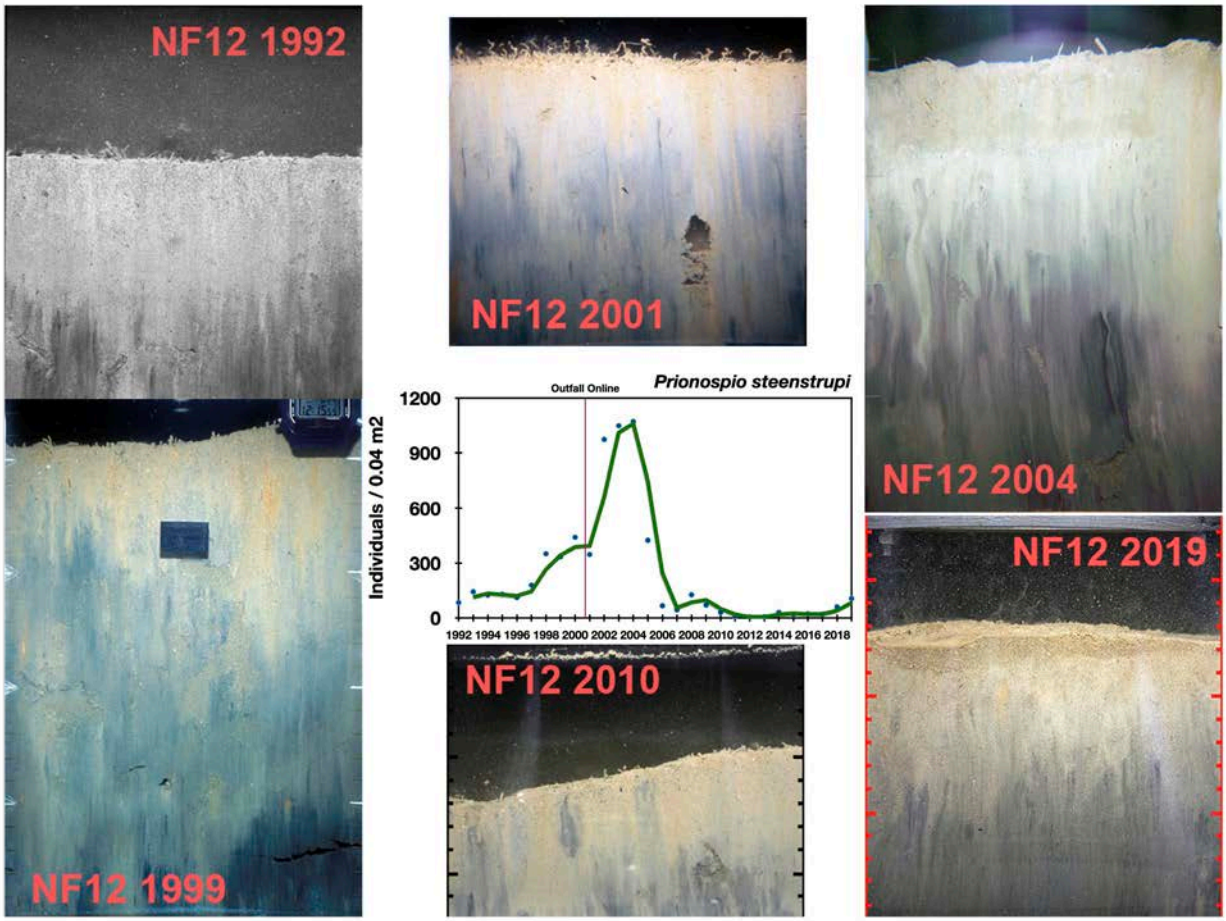

Figure 3-34 Abundance of Prionospio steenstrupi at mixed sediment Station NF12.

Species-Sediment Relationships

There is a strong association between infaunal community structure and sediment parameters, so much so that most community structure pattern can be accounted for by sediment properties. See early reviews by Gray (1974), Snelgrove and Butman (1994), Rhoads (1974), and Pearson and Rosenberg (1978). But other physical (storms, Voorhies et al. 2018) and biological factors (predation, competition, and recruitment, Peterson 1982, Woodin 1991) also play a role in determining community structure.

At the 23 nearfield stations sediments ranged from silt (NF12) to coarse sand (NF17), with a continuum of sediment characteristics in-between these two stations (Figure 3-35). Given the strong correlations between median grain-size (Phi) and percent fines (silt+clay) and percent total organic carbon (TOC) over the 28 years, percent fines was used to examine infaunal patterns (Table 3-6, Figure 3-36). The top 6 dominant species at Station NF12 were selected to represent species that prefer muddy sediments and for sandy stations, the top 6 dominants at Station NF17. Overall, correlations of abundance with percent fines and median Phi were higher than correlations with organic carbon (Table 3-7). These 12 species were 66% of all individuals collected at all 23 stations. Generally, polychaetes dominated mud stations but at sand stations dominants also included amphipods and a bivalve. The polychaete *Prionospio steenstrupi* alone accounted for over 25% of all individuals collected at the 23 stations. The most abundant non-polychaete was the amphipod *Crassicorophium crassicorne*, which made up about 2% of all individuals collected.

Species dominant at fine-sand to muddy stations tended to be broadly distributed across all nearfield stations (Figure 3-37) while those dominant at medium- and coarse-sand stations tended not to occur at stations with percent fines >20% (Figure 3-38). Mud species had their lowest abundance when percent fines was <10%. Within and between station variation in abundance of dominant muddy species through time tended to be greater than abundance variation related to percent fines. For example, *Prionospio steenstrupi* abundance was variable through time and between stations, but its abundance was not related to percent fines (Table 3-7). Abundance of *Prionospio steenstrupi* did tend to be lower with higher winter-period storm intensity (Figure 3-33). The abundance of *Mediomastus californiensis* and *Levinsenia gracilis* was more closely related to variation in percent fines than to year to year trends. Abundance of sand dominants (*Parvicardium pinnulatum, Polygordius jouinae, Spiophanes bombyx*, and *Exogone hebes*) also tended to be more a function of percent fines than of year sampled.

The relationships between species abundance and time is complicated by interaction with climate and also by small-scale variation in grain-size within a station. Through time, storms have increased in number and intensity, which has led to a coarsening of median grain-size (Figures 3-22 and 3-25). There has also been an overall decline in percent fines through time (exponential regression, $R^2 = 0.34$, $p = 0.001$) but it was not directly related to storm parameters. And despite percent fines being highly correlated to median Phi (Table 3-6), the temporal change in percent fines was not similarly correlated. Within station variability in median grain-size ranged from <10% CV at silty stations NF08 and NF12 to over 700% CV at coarse-sand Station NF18.

Table 3-6. Correlation (r) of sediment parameters for all 23 stations over the 28 years of monitoring. Sample size was 417 station*year combinations.

	% Fines	% TOC
Median Phi	0.88	0.61
% Fines		0.76

Table 3-7. Correlation (r) of the six top muddy sediment dominant species and six top sandy sediment dominants with sediment parameters. Data from all 23 stations over the 28 years of monitoring were used. Correlations >0.30 are in bold.

Species	Major Taxa	Sediment Preference	Overall Species Rank	Overall Total Individuals	% Total	Correlation (r) to total abundance[a]		
						% Fines	% TOC	Median Phi
						N = 447	N = 446	N = 417
Prionospio steenstrupi	Polychaete	Mud	1	320,398	25.7	0.06	0.13	0.03
Mediomastus californiensis	Polychaete	Mud	2	126,568	10.2	**0.61**	**0.53**	**0.50**
Aricidea catherinae	Polychaete	Mud	3	89,296	7.2	-0.04	0.09	-0.17
Tharyx acutus	Polychaete	Mud	4	86,894	7.0	0.21	0.17	0.18
Spio limicola	Polychaete	Mud	5	73,230	5.9	0.30	0.25	**0.38**
Levinsenia gracilis	Polychaete	Mud	7	33,222	2.7	**0.52**	**0.31**	**0.43**
Exogone hebes	Polychaete	Sand	8	32,592	2.6	**-0.48**	**-0.34**	**-0.45**
Crassicorophium crassicorne	Amphipod	Sand	11	23,517	1.9	-0.29	-0.26	-0.18
Spiophanes bombyx	Polychaete	Sand	18	16,044	1.3	**-0.33**	-0.30	-0.25
Polygordius jouinae	Polychaete	Sand	22	11,170	0.9	**-0.35**	**-0.32**	-0.27
Parvicardium pinnulatum	Bivalve	Sand	27	7,727	0.6	**-0.32**	-0.25	-0.24
Pseudunciola obliquua	Amphipod	Sand	54	3,329	0.3	-0.14	-0.14	-0.07

[a] abundance of each species at each station for each year compared to fines, TOC and median Phi size measured at each station for each year. Max sample size (N) is 447. TOC was not measured at NF14 in 2000 and median Phi was not calculated 1992 or 1993.

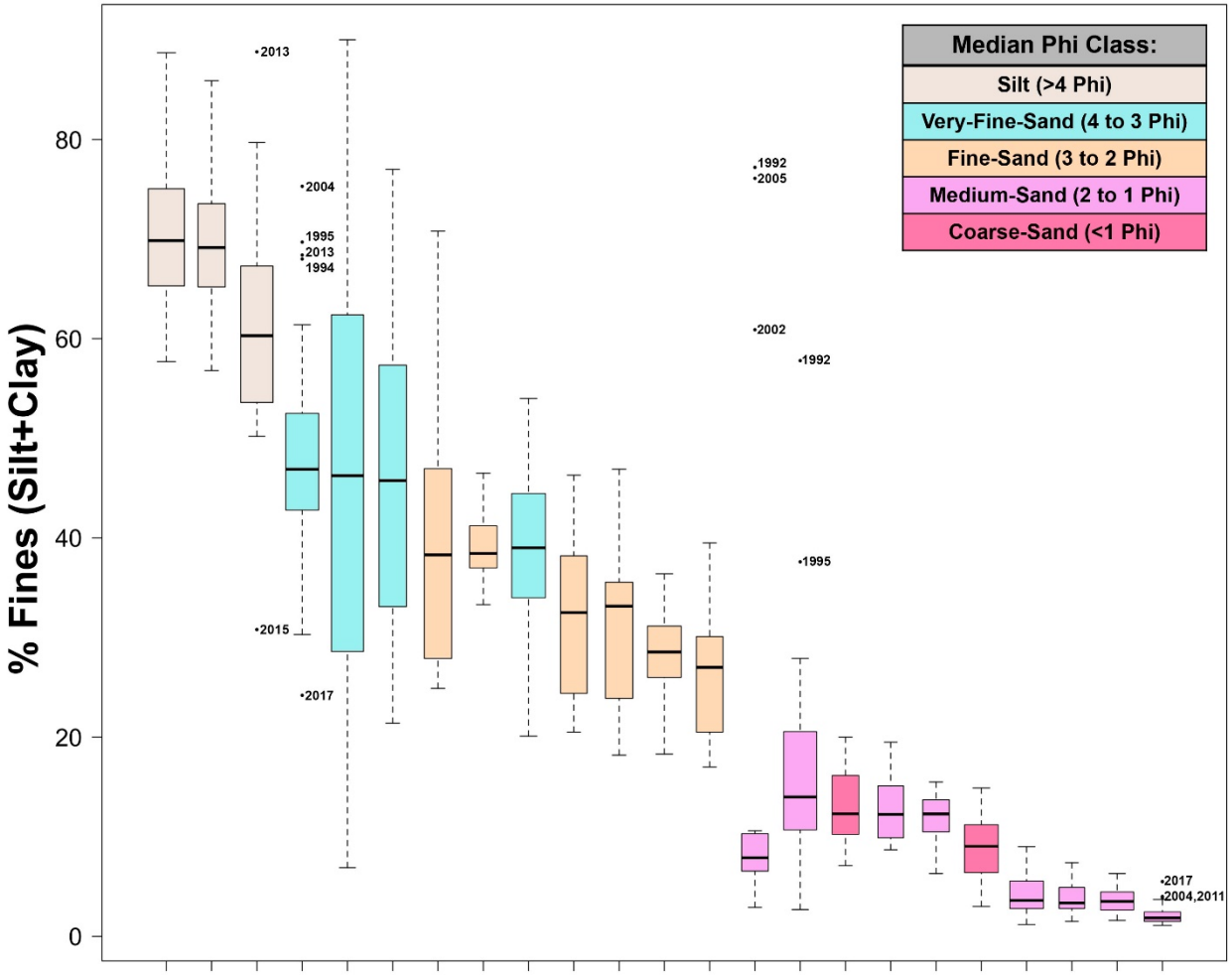

	NF12	NF08	NF21	NF22	NF24	NF16	FF13	NF09	NF10	NF07	FF10	FF12	NF05	NF02	NF20	NF18	NF15	NF19	NF14	NF04	NF23	NF13	NF17
Median Phi	4.4	4.3	4.0	3.3	3.3	3.0	2.8	2.9	3.0	2.5	2.7	2.7	2.2	1.9	1.0	0.2	1.7	1.9	0.4	1.6	1.3	1.3	1.4
SD	0.3	0.3	0.5	0.8	1.3	1.0	1.0	0.6	0.3	0.5	0.5	0.5	0.2	1.2	1.0	1.5	0.5	0.3	1.2	0.3	0.2	0.4	0.3
CV	7	6	12	24	40	34	35	20	11	22	20	18	10	60	98	772	29	18	293	22	18	32	23
TOC %	1.3	1.6	1.1	1.0	1.0	1.2	0.9	0.7	0.7	0.8	0.6	0.5	0.7	0.5	0.5	0.6	0.6	0.4	0.8	0.1	0.2	0.1	0.1
SD	0.5	0.7	0.3	0.3	0.6	0.5	0.4	0.3	0.2	0.3	0.1	0.1	0.3	0.8	0.3	0.2	0.4	0.1	0.7	0.1	0.1	0.1	0.1
CV	35	41	32	32	61	38	40	52	32	30	15	26	38	146	53	40	58	29	83	84	41	66	96

Figure 3-35 Percent fines at nearfield stations for all years (1991 to 2019) arranged from highest to lowest. Boxes are interquartile range (IR) with the central line at the median, whiskers are 2IR, outliers are labeled. Colors are the median Phi size-class, also shown on table below the graph are station means for all years.

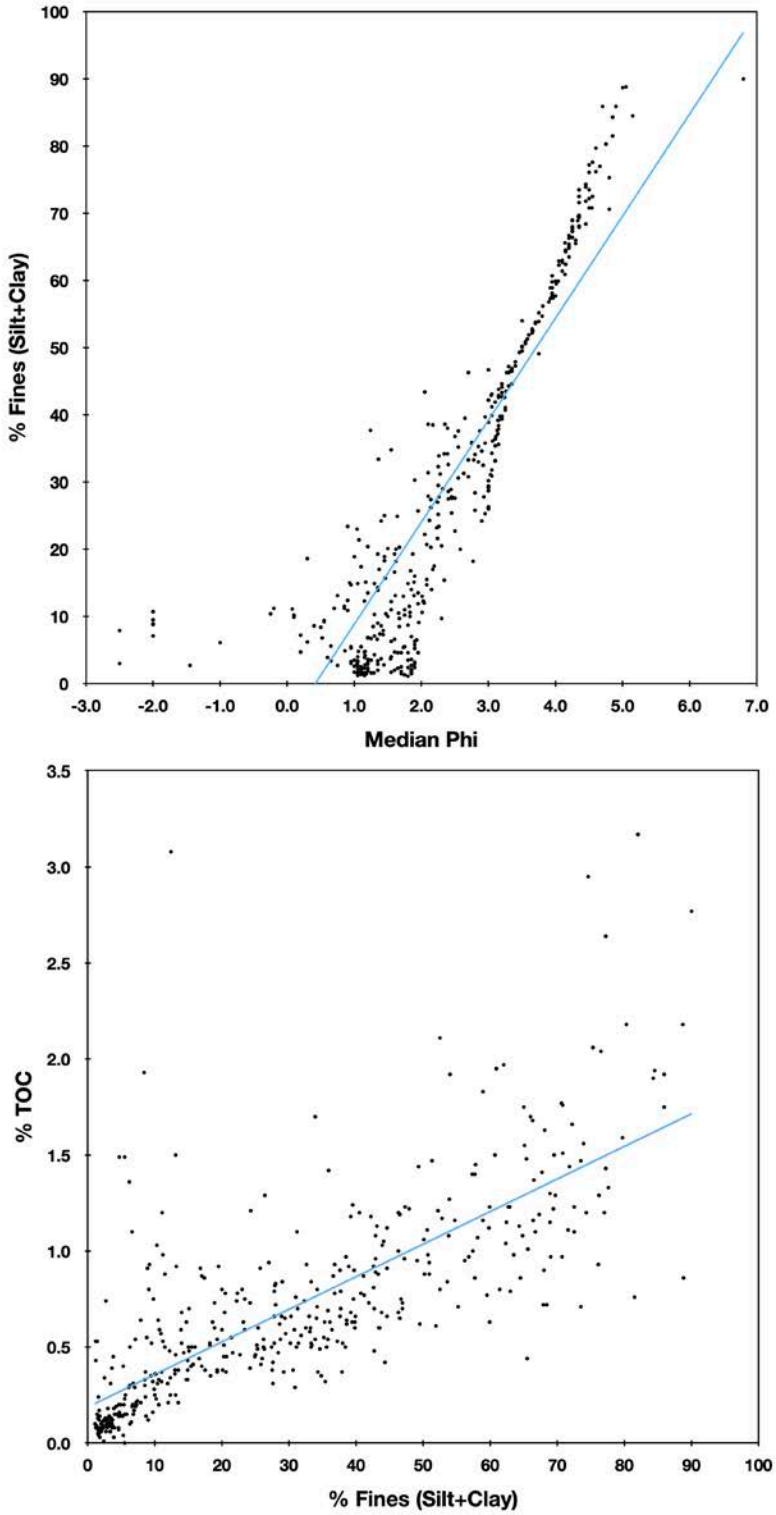

Figure 3-36 Relationship between percent fines, median Phi, and total organic carbon (TOC) for all nearfield station-year combinations.

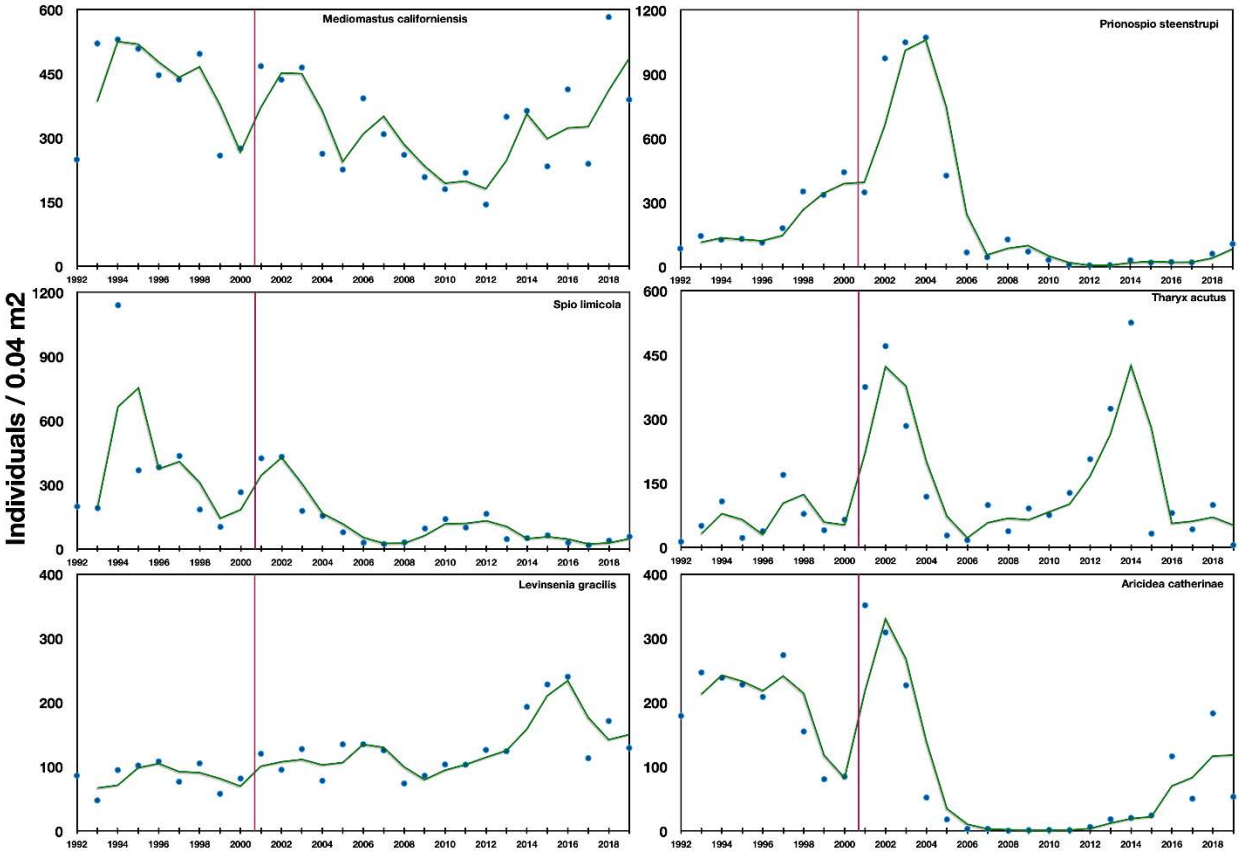

Figure 3-37 Abundance of six top dominants at muddy stations. Stations are arranged from highest to lowest percent fines (silt+clay). SPI images show sediment characteristics for 2019. Scale on side of image is in cm.

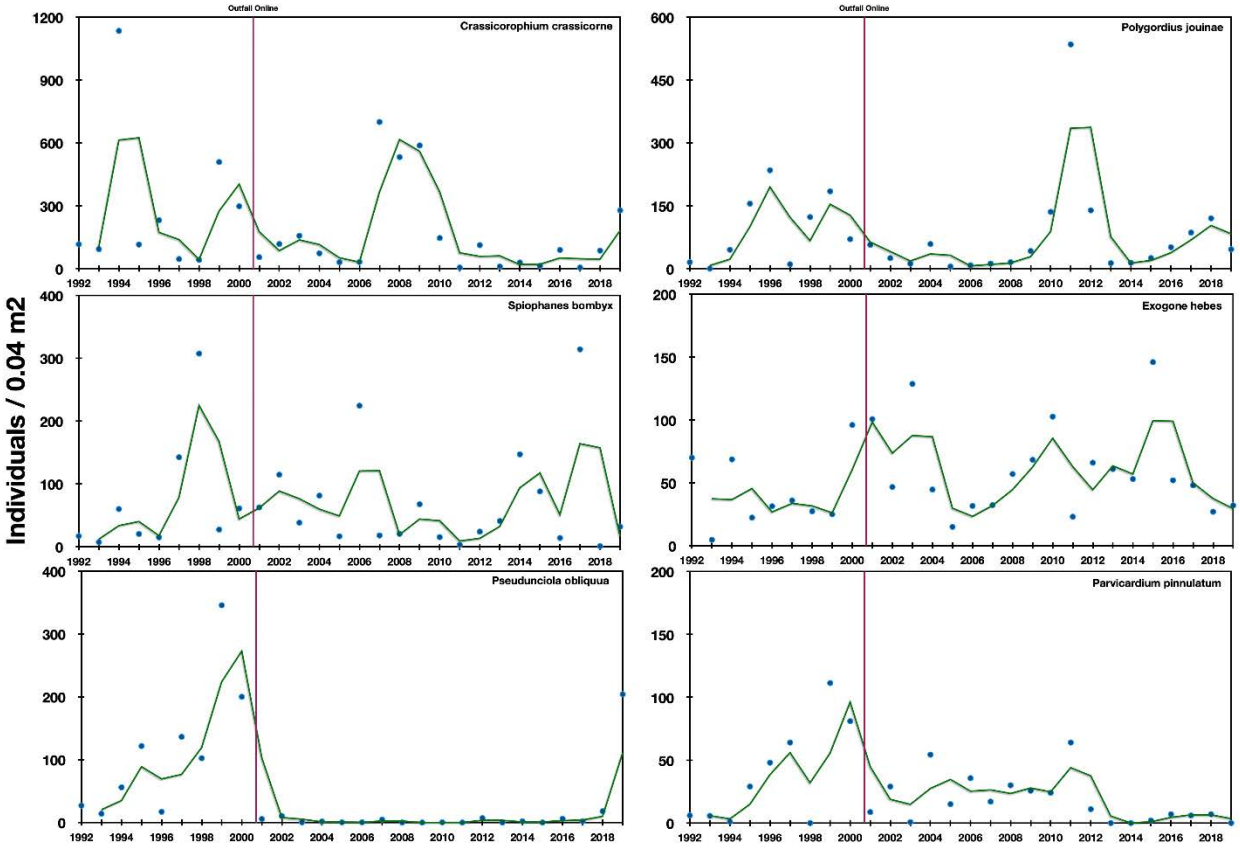

Figure 3-38 Abundance of six top dominants at sand (medium-to coarse-sand) stations. Stations are arranged from highest to lowest percent fines (silt+clay). SPI images show sediment characteristics for 2019. Scale on side of image is in cm.

Summary

There continues to be no evidence of an outfall effect on infaunal benthic habitat quality based on sediment profile imaging (SPI) data for 2019. Being among the highest annual averages for post outfall monitoring, the grand mean apparent color redox-potential discontinuity (aRPD) layer depth in 2019 did not exceed the threshold of a 50% decrease from the baseline conditions. If only measured values are considered the thickness of the aRPD for 2019 would be 4.8 cm (SD = 0.8 cm, 15 stations in mean). This is more than double the baseline aRPD layer depth average of 2.2 cm (SD = 0.48 cm).

The long-term monitoring program (1992 to 2019) at the outfall has documented change in benthic habitat quality and infaunal communities that are related to increasing storminess, which is likely related to broader effects of climate change. There was a shift from biological to physical dominance of surface sediments bed roughness, which was related to the intensity and number of winter-period storms. Sediments at many stations also coarsened during stormiest years.

In general, monitoring data point to physical processes, such as storms and storm-induced sediment transport, rather than biological processes as the primary stressors in the nearfield. Storms effect benthic ecosystems through transfer of energy to the bottom, which can resuspend and transport sediments. This physical disturbance acts on both benthic habitats and communities directly through sediment instability and by changing grain-size. Physical dominance is evident even during years when storms were not numerous or intense in the preceding winter. As a result, there are no indications of an environmental response in the benthic habitat to the offshore discharge.

Benthic habitats and communities now appear sensitive to climate variability. It is likely that climate will continue to be a prominent force for change in the future through its influence on wind and waves, hydrodynamics, salinity, and temperature.

4 SUMMARY OF RELEVANCE TO MONITORING OBJECTIVES

Benthic monitoring for MWRA's offshore ocean outfall focused on addressing three primary concerns regarding potential impacts to the benthos from the wastewater discharge: (1) eutrophication and related low levels of dissolved oxygen; (2) accumulation of toxic contaminants in depositional areas; and (3) smothering of animals by particulate matter.

Results of the SPI survey provide important insight into the question of eutrophication and dissolved oxygen. As has been noted throughout the post-diversion period, the 2019 SPI survey continued to find no indication that the wastewater discharge has resulted in lower levels of dissolved oxygen or increased deposition of organic matter in nearfield sediments. The average thickness of the sediment oxic layer in 2019 was greater than reported during the baseline period. The SPI results continued to suggest a trend towards a predominance of a pioneering stage benthic community, likely a result indicative of increased physical stress on the community. There is no evidence that the source of this stress is organic pollution; for example the infaunal study found that the numbers of opportunistic species remained negligible in 2019. The source of stress appears to be associated with storms in Massachusetts Bay that cause resuspension of bottom sediments.

The findings also support MWRA’s recommendation to regulatory agencies and their Outfall Monitoring science Advisory Panel (OMSAP) that the SPI study in Massachusetts Bay had answered its monitoring questions fully and could be ended. OMSAP endorsed this recommendation at their October 3, 2019 meeting.

Assessments in this report strongly support previous findings that the trend seen in the SPI survey likely results from the coarsening of sediment grain-size caused by sediment mixing and transport associated with storms that caused a decline in visible biogenic structures in the images. These results support previous findings that eutrophication and the associated decrease in oxygen levels have not been a problem at the nearfield benthic monitoring stations (Rutecki et al. 2019, Maciolek et al. 2008). The outfall is located in an area dominated by hydrodynamic and physical factors, including tidal and storm currents, turbulence, and sediment transport (Butman et al. 2008). Storm events significant enough to impact bottom sediments in Massachusetts Bay are common. Further, there is substantial evidence that storm impacts on nearfield sediments and benthos may have increased since the start of monitoring. These physical factors, along with the high quality of the effluent discharged into the Bay (Taylor 2010), are the principal reasons that benthic habitat quality has remained high in the nearfield area.

Surveys of soft-bottom benthic communities continue to suggest that animals near the outfall have not been smothered by particulate matter from the wastewater discharge or experienced stress resulting from increased deposition of organic matter. The percentage of fine grain sediments has not increased in the nearfield stations since the diversion indicating no pattern of settlement of particulate matter from the discharge. There were no Contingency Plan threshold exceedances for any infaunal diversity measures in 2019.

Benthic monitoring results continued to indicate that the three potential impacts of primary concern (decreased oxygen; accumulation of contaminants; and particulate deposition that smothers the benthos) have not occurred at the MWRA stations. Results also continue to demonstrate that the benthic monitoring program comprises a sensitive suite of parameters that can detect both the influence of the outfall and the subtle natural changes in benthic communities. The spatial extent of particulate deposition from the wastewater discharge is measurable in the *Clostridium perfringens* concentrations in nearfield sediments. *C. perfringens* concentrations provide evidence of the discharge footprint at stations close to the outfall. Within this footprint, no other changes to sediment composition and infaunal communities have been detected. Nonetheless, subtle variations in the species composition of infaunal assemblages clearly delineate natural spatial variation in the benthic community based on habitat (e.g., associated with different sediment grain sizes) and bottom energy (e.g., turbulance and sediment transport associated with storm events). Changes over time have also been detected including region-wide shifts in diversity, with peaks from 2010 to 2012, in the Massachusetts Bay infaunal assemblages. Detection of these spatial and temporal patterns in the benthos suggests that any ecologically significant adverse impacts from the outfall would be readily detected by the monitoring program, if those impacts had occurred.

5 REFERENCES

Agresti A. 1990. Categorical data analysis. New York: Wiley. 558 p.

Ballerstedt S. 2005. Parvicardium pinnulatum A cockle. In: Tyler-Walters H. and Hiscock K. (eds) Marine Life Information Network: Biology and Sensitivity Key Information Reviews. https://www.marlin.ac.uk/species/detail/1636.

Bothner MH, Casso MA, Rendigs RR, Lamothe PJ. 2002. The effect of the new Massachusetts Bay sewage outfall on the concentrations of metals and bacterial spores in nearby bottom and suspended sediments. Marine Pollution Bulletin. 44: 1063-1070.

Butman B, Sherwood CR, Dalyander PS. 2008. Northeast storms ranked by wind stress and wave-generated bottom stress observed in Massachusetts Bay, 1990–2006. Continental Shelf Research 28:1231–1245.

Chapman PM, Paine MD, Arthur AD, Taylor LA. 1996. A triad study of sediment quality associated with a major, relatively untreated marine sewage discharge. Marine Pollution Bulletin 32:47-64.

Clarke KR. 1993. Non-parametric multivariate analyses of changes in community structure. Aust. J. Ecol., 18: 117-143.

Clarke KR, Green RH. 1988. Statistical design and analysis for a 'biological effects' study. Mar. Ecol. Prog. Ser., 46: 213-226.

Codiga, D., S. Dalyander, and K. Keay (2019) Integrated wind and wave stresses reveal long-term increases in Gulf of Maine storminess. Gulf of Maine 2050 International Symposium, Abstract Booklet, p28. Gulf of Maine Research Institute.

Constantino J, Leo W, Delaney MF, Epelman P, Rhode S. 2014. Quality assurance project plan (QAPP) for sediment chemistry analyses for harbor and outfall monitoring, Revision 4 (February 2014). Boston: Massachusetts Water Resources Authority. Report 2014-02. 53 p.

Diaz RJ, Rhoads DC, Blake JA, Kropp RK, Keay KE. 2008. Long-term trends in benthic habitats related to reduction in wastewater discharges to Boston Harbor. Estuaries and Coasts 31:118–1197.

Draper, NR, Smith H. 1998. Applied regression analysis (Vol. 326). John Wiley & Sons.

Elías R, Palacios JR, Rivero MS, Vallarino EA. 2005. Short-term responses to sewage discharge and storms of subtidal sand-bottom macrozoobenthic assemblages off Mar del Plata City, Argentina (SW Atlantic). Journal of Sea Research 53:231-42.

Foulquier C, Baills J, Arraud A, D'Amico F, Blanchet H, Rihouey D, Bru N. 2020. Hydrodynamic conditions effects on soft-bottom subtidal nearshore benthic community structure and distribution. Journal of Marine Sciences. https://doi.org/10.1155/2020/4674580

Fulweiler RW, Nixon SW. 2009. Responses of benthic-pelagic coupling to climate change in a temperate estuary. Hydrobiologia 629:147–156

Gray JS. 1974. Animal-sediment relationships. Oceanography and Marine Biology Annual Review 12:223-261.

Hilbig B, Blake JA. 2000. Long-term analysis of polychaete-dominated benthic infaunal communities in Massachusetts Bay, USA. Bulletin of marine science 67:147-164.

Janssen F, Huettel M, Witte U. 2005. Pore-water advection and solute fluxes in permeable marine sediments (II): Benthic respiration at three sandy sites with different permeabilities (German Bight, North Sea). Limnology and Oceanography 50:779-792.

Kröncke I, Dippner JW, Heyen H, Zeiss B. 1998. Long-term changes in macrofaunal communities off Norderney (East Frisia, Germany) in relation to climate variability. Marine Ecology Progress Series 167:25-36.

Labrune C, Grémare A, Guizien K, Amouroux JM. 2007. Long-term comparison of soft bottom macrobenthos in the Bay of Banyuls-sur-Mer (north-western Mediterranean Sea): a reappraisal. Journal of Sea Research 58:125-143.

Libby PS, Borkman DG, Geyer WR, Turner JT, Costa AS, Wang J, Codiga D. 2019. 2018 Water Column Monitoring Results. Boston: Massachusetts Water Resources Authority. Report 2019-08. 52p.

Maciolek NJ, Diaz RJ, Dahlen DT, Hecker B, Williams IP, Hunt CD, Smith WK. 2007. 2006 Outfall benthic monitoring report. Boston: Massachusetts Water Resources Authority. Report 2007-08. 162 p.

Maciolek NJ, Doner SA, Diaz RJ, Dahlen DT, Hecker B, Williams IP, Hunt CD, Smith W. 2008. Outfall Benthic Monitoring Interpretive Report 1992–2007. Boston: Massachusetts Water Resources Authority. Report 2008-20. 149 p.

Mermillod-Blondin F, Rosenberg R. 2006. Ecosystem engineering: the impact of bioturbation on biogeochemical processes in marine and freshwater benthic habitats. Aquatic Sciences 68:434-442.

Morgan MA, Woodhead PMJ. 1984. The life history and sexual biology of *Pseudunciola obliquua* (crustacea: amphipoda) in the New York Bight. Estuarine, Coastal and Shelf Science 18:639-650.

MWRA. 1991. Massachusetts Water Resources Authority effluent outfall monitoring plan phase I: baseline studies. Boston: Massachusetts Water Resources Authority. Report 1991-ms-02. 95 p.

MWRA. 1997. Massachusetts Water Resources Authority Contingency Plan. Boston: Massachusetts Water Resources Authority. Report 1997-ms-69. 41 p.

MWRA. 2001. Massachusetts Water Resources Authority Contingency Plan Revision 1. Boston: Massachusetts Water Resources Authority. Report ENQUAD ms-071. 47 p.

MWRA. 2004. Massachusetts Water Resources Authority Effluent Outfall Ambient Monitoring Plan Revision 1, March 2004. Boston: Massachusetts Water Resources Authority. Report 1-ms-092. 65 p.

MWRA. 2010. Ambient monitoring plan for the Massachusetts Water Resources Authority effluent outfall revision 2. July 2010. Boston: Massachusetts Water Resources Authority. Report 2010-04. 107p.

Nestler EC, Diaz RJ, Hecker B. 2018. Outfall Benthic Monitoring Report: 2017 Results. Boston: Massachusetts Water Resources Authority. Report 2018-05. 57 p. plus Appendices.

Odum EP. 1969. The strategy of ecosystem development. Science 164:262-270.

Pearson TH, Rosenberg R. 1978. Macrobenthic succession in relation to organic enrichment and pollution of the marine environment. Oceanography and Marine Biology: An Annual Review 16:229-311.

Peterson CH. 1982. The importance of predation and intra-and interspecific competition in the population biology of two infaunal suspension-feeding bivalves, *Protothaca staminea* and *Chione undatella*. Ecological Monographs 52:437-475.

Puente A, Diaz RJ. 2015. Response of benthos to ocean outfall discharges: does a general pattern exist? Marine Pollution Bulletin 101:174-81.

Reguero BG, Losada IJ, Méndez FJ. 2019. A recent increase in global wave power as a consequence of oceanic warming. Nature communications 10:1-14.

Rhoads DC. 1974. Organism sediment relations on the muddy sea floor. Oceanography and Marine Biology Annual Review 12:263-300.

Rhoads DC, Germano JD. 1986. Interpreting long-term changes in benthic community structure: A new protocol. Hydrobiologia 142:291-308.

Rutecki DA, Nestler EC, Hasevlat RC. 2017. Quality Assurance Project Plan for Benthic Monitoring 2017–2020. Boston: Massachusetts Water Resources Authority. Report 2017-06, 92 p. plus Appendices.

Rutecki DA, Diaz RJ, Nestler EC, Codiga DL, Madray ME. 2019. 2018 Outfall Benthic Monitoring Results. Boston: Massachusetts Water Resources Authority. Report 2019-06. 59 p.

Signell RP, Butman B. 1992. Modeling tidal exchange and dispersion in Boston Harbor. Journal of Geophysical Research 97:15591–16606.

Signell RP, Jenter HL, Blumberg AF. 2000. Predicting the physical effects of relocating Boston's sewage outfall. Estuarine, Coastal and Shelf Science 50:59-71.

Snelgrove PVR, Butman CA. 1994. Animal-sediment relationships revisited: cause versus effect. Oceanography and Marine Biology Annual Review 32:111–177.

Solan M, Kennedy R. 2002. Observation and quantification of in situ animal-sediment relations using time-lapse sediment profile imagery (t-SPI). Marine Ecology Progress Series 228:179-191.

Talke SA, Kemp AC, Woodruff J. 2018. Relative sea level, tides, and extreme water levels in Boston Harbor from 1825 to 2018. Journal of Geophysical Research: Oceans 123:3895-3914.

Taylor DI. 2010. The Boston Harbor Project, and large decreases in loadings of eutrophication-related materials to Boston Harbor. Marine Pollution Bulletin 60:609–619.

Thompson CEL, Williams ME, Amoudry L, Hull T, Reynolds S, Panton A, Fones GR. 2017. Benthic controls of resuspension in UK shelf seas: implications for resuspension frequency. Continental Shelf Research. (doi:10.1016/j.csr.2017.12.005).

Trueblood DD, Gallagher ED, Gould DM. 1994. Three stages of seasonal succession on the Savin Hill Cove mudflat, Boston Harbor. Limnology and Oceanography 39:1440-1454.

Turner JT, Borkman DG, Hunt CD. 2006. Zooplankton of Massachusetts Bay, USA, 1992–2003: relationships between the copepod *Calanus finmarchicus* and the North Atlantic Oscillation. Marine Ecology Progress Series 311:115-124.

United States Global Change Research Program (USGCRP). 2017. Climate Science Special Report: Fourth National Climate Assessment, Volume I [Wuebbles DJ, DW Fahey, KA Hibbard, DJ Dokken, BC Stewart, TK Maycock (eds.)]. U.S. Global Change Research Program, Washington, DC, USA, 470 pp., doi: 10.7930/J0J964J6.

Voorhies KJ, Wootton JT, Henkel SK. 2018. Longstanding signals of marine community structuring by winter storm wave-base. Marine Ecology Progress Series 603:135-146.

Warner JC, Butman B, Dalyander PS. 2008. Storm-driven sediment transport in Massachusetts Bay. Continental Shelf Research 28:257-282.

Warwick RM. 1993. Environmental impact studies on marine communities: pragmatical considerations. Aust. J. Ecol., 18: 63-80.

Werme C, Keay KE, Libby PS, Codiga DL, Charlestra L, Carroll SR. 2019. 2018 outfall monitoring overview. Boston: Massachusetts Water Resources Authority. Report 2019-07. 53 p.

Woodin SA. 1991. Recruitment of infauna: positive or negative cues? American Zoologist 31:797-807.

Massachusetts Water Resources Authority
100 First Avenue • Boston, MA 02129
www.mwra.com
617-242-6000